

1 An approach for VLE model development, validation, and implementation in Aspen 2 Plus for amine blends in CO₂ capture: the HS3 solvent case study

3 Matteo Gilardi^{1a,*}, Filippo Bisotti^{2a,*}, Andrew Tobiesen², Hanna K. Knuutila³, Davide Bonalumi¹

4 ¹ Politecnico di Milano- Department of Energy, via Lambruschini 4A, 20156, Milano, Italy.

5 ² SINTEF Industry – Process Technology, KPMT - Kjemisk prosess og miljøteknologi, Richard Birkelands vei 3, 7034, Trondheim, Norway

6 ³ Department of Chemical Engineering, Norwegian University of Science and Technology, NTNU, Trondheim, NO-7491, Norway

7 ^a authors equally contribute to the research activity presented in this work

8 *corresponding authors – matteo.gilardi@polimi.it; filippo.bisotti@sintef.no

9

10 Abstract

11 Carbon Capture and Storage (CCS) using chemical absorption is a viable method to significantly cut CO₂
12 emissions in the industrial and energy sectors. However, further development of improved absorbents is
13 necessary to reduce the costs and environmental impact of current CCS technologies. To design the process
14 and quantify energy consumption and costs through process simulation, it is necessary to implement an
15 accurate and robust thermodynamic model. This article describes in details how to develop, regress, and
16 validate a VLE model using ELECNRTL model in Aspen Plus V11 for the novel HS3 solvent, a blend of 3-amino-
17 1-propanol and 1-(2-hydroxyethyl) pyrrolidine, which is currently being characterized in Realise (H2020-
18 funded project). The VLE model is validated over a wide range of temperatures and loadings. The proposed
19 procedure to regress ELECNRTL parameters can be used as a general guideline for implementing VLE models
20 in Aspen Plus for generic amine blends or electrolyte solutions.

21

22 Highlights

- 23 • Aspen Plus VLE model implementation approach for AP-PRLD blend for CO₂ capture
- 24 • The methodology is general and applicable for developing ELECNRTL models
- 25 • Experimental validation using quality in-house VLE data
- 26 • Accurate estimation of absorption heat and reasonable speciation plots are obtained
- 27 • Estimation of physical properties of the blend

28

29 **Keywords:** amine blends, CO₂ capture, ELECNRTL Aspen Plus, equilibrium model, model validation, chemical
30 absorption.

31

32 1. INTRODUCTION

33 Carbon capture and storage (CCS) is considered a key technology in reducing global carbon dioxide emissions.
34 Considering that industrial sources account for about 16% of the worldwide CO₂ emissions (epa.gov, 2022),
35 installing CO₂ removal facilities to treat the flue gas from those production plants, such as refineries and
36 cement plants, can play a key role in mitigating climate changes. However, the current implementation of
37 CCS technologies at the industrial level is limited, mainly due to high costs (Yamada, 2021). The significant
38 thermal duties required to regenerate conventional amine solvents, such as mono-ethanolamine (MEA) and
39 methyl-diethanolamine (MDEA) may therefore be a limitation for global implementation and deployment. It
40 is, therefore, essential to further improve the efficiency of the overall process by developing innovative
41 solvents with improved capture capacity and lower environmental impact compared to traditional amines

42 used for CO₂ absorption (Pellegrini et al., 2021). A new aqueous amine blend (the HS3 solvent) which is made
43 up of a primary polyamine (3-amino-1-propanol, named AP) at 15 wt%, and a tertiary amine (1-(2-
44 hydroxyethyl) pyrrolidine, named PRLD) at 40 wt% concentration, has been characterized as part of the
45 Realise project funded by the European Community (Realise, 2022). The experimental tests carried out so far
46 have shown that the CO₂ cyclic capacity of HS3 can be significantly higher than that of 30 wt% MEA.
47 Preliminary analysis indicates that the solvent has a significantly lower regeneration duty compared to the
48 benchmark MEA solvent. An elaborate pilot campaign is also currently being carried out at the Tiller plant
49 (September 2022 - January 2023 in Trondheim, Norway).

50 The development and validation of first-principle models are essential to accurately model and simulate
51 advanced chemical processes. Such simulation models are used as an important tool for energy-, cost- and
52 design calculations in several fields of chemical- and energy engineering (Bisotti et al., 2022, 2021; Kucka et
53 al., 2003; Liu et al., 2016; Svendsen et al., 2011).

54 This article presents a procedure to develop and validate an eNRTL (ELECRTL) VLE model of the Realise HS3
55 solvent, implemented in Aspen Plus V11 (Aspen Plus®, 2019; Liu et al., 2016). Ancillary models that describe
56 physical properties such as density, viscosity, and heat capacity are provided, as well as the definition of the
57 chemical reaction scheme during CO₂ absorption together with the temperature-dependent equilibrium
58 constants. The developed model has been validated in the temperature range from 40 to 120°C, and for
59 solvent CO₂ loadings from 0.01 up to 1 mol/mol. Uncertainty analysis has been conducted, investigating the
60 model's accuracy against the measured VLE data.

61 The proposed approach provides a general methodology of implementation, which has not been published
62 earlier. The proposed general approach can, be applied to any ELECRTL activity coefficients model. The
63 authors would like to remark that the VLE correct representation and prediction is at the base of any capture
64 system, and it affects the design of the two main units (i.e., absorber and regenerator), as well as all other
65 units that require the calculation of the phase equilibrium (i.e., flashes). Details concerning physical property
66 models available in Aspen Plus V11 and the way they are referred to and named in the process simulator are
67 highlighted so that the article can be considered as a detailed implementation guideline to construct an
68 ELECRTL model in Aspen Plus for reactive liquid-gas systems, such as amine blends used to capture CO₂.
69 The supplemental solvent physical properties and the corresponding models describing these properties are
70 reported in the Supplementary Material.

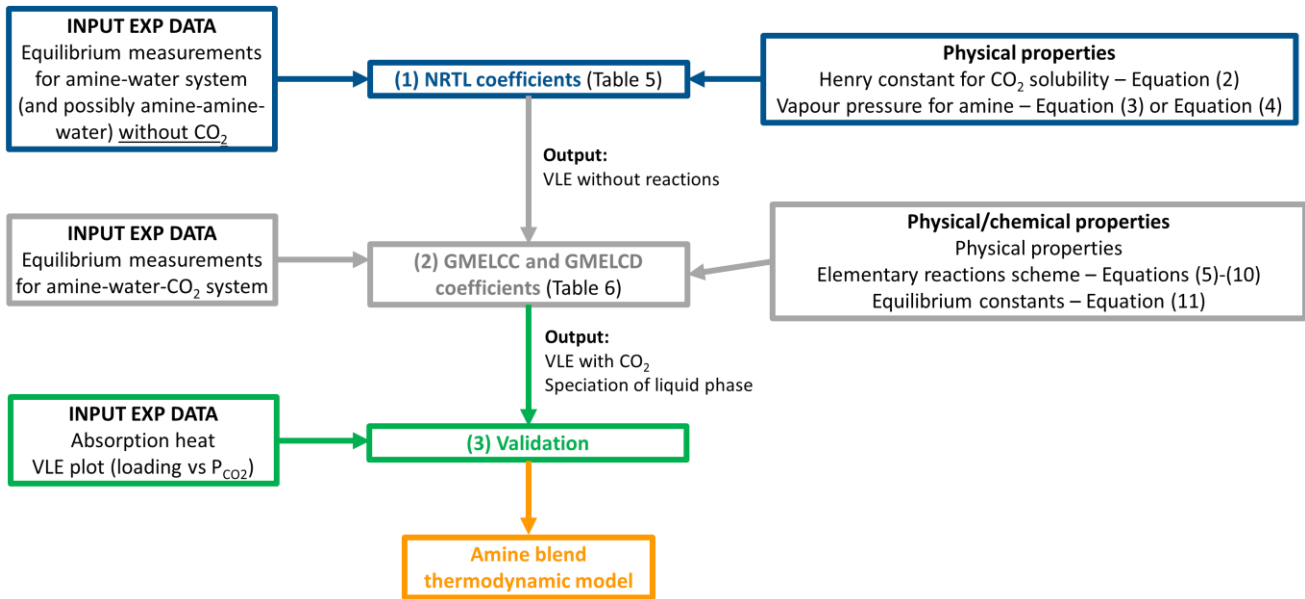
71

72 **2. METHODS**

73 An ELECRTL model is exploited to describe the interactions in the liquid phase in HS3 solvent, while the gas
74 phase is simply modelled as an ideal gas (Antoine equation), in accordance with the theoretical background
75 paragraph (Aspen Plus®, 2019). This approach has already been implemented with successful results for
76 many standard amine-based solvents and it is still the most widely used commercial suite for simulating
77 processes based on mono-ethanolamine (MEA) and methyl-diethanolamine (MDEA). The main steps
78 required to build an ELECRTL model for a new blend are represented in the flowchart of Figure 1. More
79 specifically, molecule-molecule interactions are firstly described disregarding the formation of ions; in a
80 further step, molecule-ions interactions are described based on the implemented elementary reaction
81 scheme by fitting dedicated ELECRTL coefficients to VLE data for complete system (amine-H₂O-CO₂).
82 Finally, the obtained VLE model must be tested to check its reliability, accuracy and stability. This diagram
83 also clarifies which are the experimental data exploited in each progressive step.

84 Table 1 gathers and lists all the parameters that should be implemented to properly define the VLE for
85 amine(s) blends. Moreover, the same table reports the references used to get experimental data and/or

86 models for some of the parameters implemented in Aspen Plus. For physical properties, please refer to the
 87 Supplementary Material.
 88
 89



90
 91
 92 **Figure 1. Flowchart summarizing the procedure followed in this work for ELECNRTL model development and validation.**

93
 94 **Table 1. List of parameters and thermodynamic properties necessary to properly define ELECNRTL model in Aspen Plus**

Property	Model name in Aspen	Parameters regressed in Aspen Plus (corresponding element in the equation)	Model expression	Data sources for fitting
Activity coefficient model (VLE model)	NRTL (molecule-molecule pairs)	NRTL/1 (A_{ij}) NRTL/1 (A_{ji}) NRTL/2 (B_{ij}) NRTL/2 (B_{ji}) NRTL/3 (α_{ij})	$\ln(\gamma_i) = \frac{\sum_{j=1}^n x_j \cdot \tau_{ji} \cdot G_{ji}}{\sum_{k=1}^n x_k \cdot G_{ki}} + \sum_{j=1}^n \frac{x_j \cdot G_{ij}}{\sum_{k=1}^n x_k \cdot G_{kj}} \cdot \left(\tau_{ij} - \frac{\sum_{m=1}^n x_m \cdot \tau_{mj} \cdot G_{mj}}{\sum_{k=1}^n x_k \cdot G_{kj}} \right)$ $G_{ji} = \exp(-\alpha_{ij} \cdot \tau_{ij})$ $\alpha_{ij} = \alpha_{ji} = \text{non randomness factor}$ $\alpha_{ij} = 0.1 \text{ (recommended default value in ELECNRTL)}$ $\tau_{ij} = A_{ij} + \frac{B_{ij}}{T}$	Binary AP-H ₂ O VLE data by: • (Bernhardsen et al., 2019)
	GMELC (molecule and ion-molecule pairs)	GMELCC (A_{ij}) GMELCC (A_{ji}) GMELCD (B_{ij}) GMELCD (B_{ji})		AP-PRLD-CO ₂ -H ₂ O data (REALISE, 2022)

Vapor pressure	Extended Antoine	PLXANT (C_1, C_2, C_3)	$\ln(P_{\text{sat}}[\text{bar}]) = C_1 + \frac{C_2}{T[\text{K}] + C_3}$	AP: • (Green and Perry, 2007) PRLD: • (Bernhardsen et al., 2019)
Henry's constant	Henry's constant	HENRY ($A_{ij}, B_{ij}, C_{ij}, D_{ij}$)	$\ln(\text{He}[\text{kPa}]) = A_{ij} + \frac{B_{ij}}{T} + C_{ij} \cdot \ln(T) + D_{ij} \cdot T$	(REALISE, 2022)
Reaction equilibrium constant		A B C D	$\ln(K_i) = A + \frac{B}{T} + C \cdot \ln(T) + D \cdot T$	AP: • (Dong et al., 2010) PRLD: • (Li et al., 2017)

95

96 2.1 Henry constant

97 In order to estimate the physical solubility of the pure i-th components, i.e, the CO₂, a Henry correlation (H_i)
98 is used. Therefore, the solubility is part of the requirement of fulfilling the vapor-liquid equilibria relationship
99 between the liquid species and fugacities (f_i^V), see section 2.4.1. For the CO₂, it is important to define this
100 parameter since the affinity between CO₂ and the pure amines and their blends depends on the amines
101 features, which affects both the physical (VLE) and the chemical equilibrium (amines speciation and amount
102 of dissolved CO₂ into the liquid).

103 Since CO₂ reacts as it contacts an amine, N₂O analogy is the only possible way to estimate the solubility
104 constants as in (1). This approach is widely adopted in the literature (Aronu et al., 2011; Bishnoi and Rochelle,
105 2000; Sada et al., 1977).

$$H_{\text{CO}_2\text{-amine}} = \frac{H_{\text{N}_2\text{O-amine}} \cdot H_{\text{CO}_2\text{-H}_2\text{O}}}{H_{\text{N}_2\text{O-H}_2\text{O}}} \quad (1)$$

106

107 N₂O solubility data in water, AP and PRLD have been collected within the Realise project in a temperature
108 range between 15°C and 80°C with a step of 5°C. Then, expression (1) was adopted to estimate the Henry
109 constant for CO₂-AP and CO₂-PRLD at every temperature. Finally, Henry's constant temperature dependence
110 is defined according to correlation (2) used in Aspen Plus.

$$\ln(\text{He}[\text{kPa}]) = A + \frac{B}{T} + C \cdot \ln(T) + D \cdot T \quad (2)$$

111

112 The values of parameters A, B, C, and D resulting from the minimization of the relative square deviations
113 between the solubility were calculated based on the experimental solubility data and the model predictions.

114

115

116

117 2.2 Vapor pressure

118 The vapor pressure describes the phase equilibrium between the aqueous solution, namely water and the
119 amine(s), and the corresponding vapor phase allowing the prediction of the amine concentration of amines
120 in the vapor phase. Correct description of vapor pressure is also important in design of the water washing
121 section abating the amine traces in the treated gas. The vapor pressure of pure AP and PRLD can be modelled
122 in Aspen Plus exploiting the extended Antoine equation, reported in (3).

$$\ln(P_{\text{sat}}[\text{bar}]) = C_1 + \frac{C_2}{T[\text{K}] + C_3} + C_4 \cdot \ln(T[\text{K}]) + C_5 \cdot T \quad (3)$$

123

124 For simplicity, a standard Antoine equation expression (4) can be adopted without losing accuracy. For
125 the sake of knowledge, the SRK equation has also been tested. The observed relative differences between
126 the partial pressure of CO₂ at given loading and operating temperature obtained with SRK and ideal gas
127 model remained always below 1%.

$$\ln(P_{\text{sat}}[\text{bar}]) = C_1 + \frac{C_2}{T[\text{K}] + C_3} \quad (4)$$

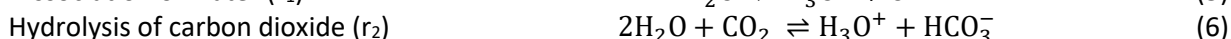
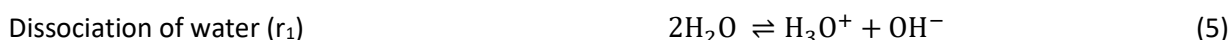
128

129 The coefficients in Antoine expression can be available in the literature or refitted from experimental data.
130 For what specifically concerns HS3, Antoine coefficients are already available in the literature for AP (Green
131 and Perry, 2007), while the coefficients for PRLD have been fitted to the vapor pressure data collected in
132 Berhardsen (Bernhardsen et al., 2019).

133

134 2.3 Elementary reaction schemes and equilibrium constants

135 Amines react with the absorbed CO₂ following well-established elementary chemical reactions. Primary
136 amine (such as AP) can speciate into the protonate form according to reaction r_4 or turn into their carbamate
137 form as in r_5 . In the latter reaction, the CO₂ is fixed into the bicarbonate ion whose formation is described in
138 reaction r_2 . Tertiary amine (such as PRLD) can only protonate or deprotonate as in r_6 . The scheme of
139 elementary reactions is complete with the self-ionization of water (r_1) and the carbonate formation (r_3). This
140 elementary scheme has already been implemented to characterize several amine blends in Aspen Plus
141 (Dutcher et al., 2015; Kucka et al., 2003; Liu et al., 2016; Yamada, 2021).



142

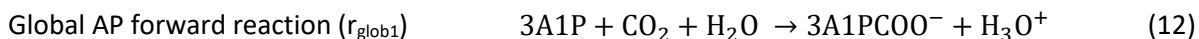
143 The equilibrium constant can be expressed as a function of the temperature as in equation (11):

$$\ln(K_i) = A + \frac{B}{T} + C \cdot \ln(T) + D \cdot T \quad (11)$$

144

145 For reactions r_1 to r_3 , which are not dependent on the specific solvent under investigation, the temperature
146 dependence of the equilibrium constant has been expressed considering literature coefficients (Posey and
147 Rochelle, 1997). For reaction r_4 the coefficients A to D have been regressed starting from the expression

148 provided in a contribution by Dong et al., 2010, where the equilibrium constant is defined as a function of
 149 both temperature and CO₂ loading. Reaction r_5 is the difference between the global reaction for AP r_{glob1} in
 150 (12) and reaction r_2 in (6).



151

152 Due to the properties of logarithms, the equilibrium constant of reaction r_5 is simply given by (13):

$$\ln (Keq_{r5}) = \ln (Keq_{glob1}) - \ln (Keq_{r2}) \quad (13)$$

153

154 The temperature dependence of the r_{glob1} reaction equilibrium constant has already been investigated by
 155 Dong et al. (Dong et al., 2010), thus we directly exploited their results. Finally, for reaction r_6 , parameters for
 156 Keq according to expression (11) have been calculated based on experimental data by (Li et al., 2017)
 157 reporting the amine protonation constant at different temperatures.

158 2.4 Theoretical background of activity-based VLE models

159 A thermodynamic VLE model is essential to define interactions between the constituents of a mixture under
 160 vapour-liquid equilibrium conditions. The selection of the most suitable model is strongly dependent on the
 161 specific system under investigation. Amine-based solvents are characterized by a strongly non-ideal liquid
 162 phase behavior, mainly due to the formation of several interacting cationic and anionic species. Conversely,
 163 the interactions in the gas phase can be neglected (i.e., ideal gas behavior and ideal gas mixture) unless the
 164 system is highly pressurized ($P > 10$ bar). The cation-anions interactions are negligible as well in the gas phase
 165 since charged molecules do not vaporize. Under these assumptions, the gas phase can be assumed close to
 166 ideal conditions, thus, a cubic equation of state, or even, the ideal gas models, are suitable for characterizing
 167 the vapor phase in equilibrium with its liquid mixture. Binary interactions in the liquid phase for a strongly
 168 non-ideal system, such as CO₂, can be adequately described through the so-called Non-Random-Two-Liquid
 169 (NRTL) model.

170 2.4.1 Chemical and phase equilibria

171 Chemical and phase equilibria model involves solving both chemical equilibria of the reactions in the liquid
 172 phase, as well as the multi-component phase equilibria. Amine systems involve both molecular species and
 173 a range of ionic species, which can make the numerical solution complex. The description of chemical
 174 reactions occurring in the system under investigation is described in section 2.3. In addition to the reaction
 175 speciation in the liquid phase, the vapor-liquid equilibria must be solved through the fundamental
 176 equilibrium criterion, which minimizes the Gibbs energy of the solution at phase equilibrium. Phase
 177 equilibrium is reached as the chemical potential (μ) of a certain species is equal in both phases (see equation
 178 (14)). Since the chemical potential can be directly linked to fugacity according to expression (15), the
 179 equilibrium can also be expressed by the equality of the fugacities (f) in the liquid and vapour phase. As a
 180 result, vapor-liquid equilibrium of a particular species i can be defined according to expression (16), when
 181 the Poynting correction factor and the non-idealities in the gas-phase are disregarded. Models based on
 182 expression (16) are called activity coefficient models since γ_i is the correction factor that is introduced to
 183 account for the molecular and cationic-anionic interactions occurring in the system.

$$\mu_i^{vap} = \mu_i^{liq} \quad (14)$$

$$d(n f_i) = \frac{d\mu}{RT} \quad (15)$$

$$P \cdot y_i = \alpha \cdot x_i \cdot \gamma_i \quad (16)$$

184

185 Where the parameter α is defined in different ways according to the single species. It corresponds to the
 186 Henry (H_i) coefficients for the CO_2 since it is highly diluted in the liquid phase, whereas it is the vapor pressure
 187 for all the other species that can be present in the gas phase (amines and water). For the gas phase the ideal
 188 gas behavior has been adopted since the estimates of the critical properties and Pitzer factor may contain
 189 large deviations affecting the predictions for the cubic equation of state. Since the equilibrium is reached at
 190 a given temperature and pressure, when the Gibbs free energy of the system is minimized, the optimal set
 191 of activity coefficients to characterize the liquid phase composition is calculated numerically by minimization
 192 following chosen reference states. When all activity coefficients approach the unity, it means that the system
 193 behaves as an ideal mixture. The higher the deviation of the system from ideality, the furthest from unity are
 194 the corresponding activity coefficient values. An adequate estimation of the activity coefficients (γ_i) is
 195 essential to define the composition of the liquid (including the forming cations and ions) in chemical and
 196 physical (global) equilibrium with the corresponding gaseous phase.

197

198 2.4.2 The e-NRTL activity coefficient model

199 The NRTL model is an activity coefficient model that correlates the activity coefficients of a compound with
 200 its mole fractions in the liquid phase (Renon and Prausnitz, 1969, 1968). It is based on the hypothesis of
 201 Wilson that the local concentration around a molecule is different from the bulk concentration, which is
 202 caused by a difference between the interaction energy of the central molecule with the molecules of its own
 203 kind and that with the molecules of the other components that are present in the system. The energy
 204 difference also introduces a non-randomness at the local molecular level, which is expressed by the
 205 parameter called non-randomness factor α .

206 The general expression of the NRTL model for determining the activity coefficient γ_i of the i -th generic species
 207 in a multicomponent mixture of n components is reported in the expressions (17) to (19) here below (Renon
 208 and Prausnitz, 1969, 1968), where τ_{ij} are the temperature-dependent parameters describing the interaction
 209 between a molecule or the ion i with another molecule or the ion j and α_{ij} is the non-randomness factor
 210 associated to the interaction of component i with component j . By definition, α_{ij} is symmetric, meaning that
 211 α_{ij} is equal to α_{ji} .

$$\ln(\gamma_i) = \frac{\sum_{j=1}^n x_j \cdot \tau_{ji} \cdot G_{ji}}{\sum_{k=1}^n x_k \cdot G_{ki}} + \sum_{j=1}^n \frac{x_j \cdot G_{ij}}{\sum_{k=1}^n x_k \cdot G_{kj}} \cdot \left(\tau_{ij} - \frac{\sum_{m=1}^n x_m \cdot \tau_{mj} \cdot G_{mj}}{\sum_{k=1}^n x_k \cdot G_{kj}} \right) \quad (17)$$

$$G_{ji} = \exp(-\alpha_{ij} \cdot \tau_{ij}) \quad (18)$$

$$\tau_{ij} = A_{ij} + \frac{B_{ij}}{T} \quad (19)$$

212

213 The NRTL method has been extended to account for cation-anion pairs with neutral molecules inside mixed
 214 solvent electrolyte systems in a wide temperature range (Chen and Song, 2004; Hartono et al., 2021; Lin et
 215 al., 2022). The ELECNRTL model is based on the same theoretical framework as the generic NRTL model, but
 216 the expression is modified compared to the original Renon and Prausnitz NRTL model. This modification
 217 introduces the like-ion repulsion and local electroneutrality assumptions (Lin et al., 2010) to provide a more
 218 representative picture of the electrical charge effects, which play a key role in amine solutions. The resulting
 219 model succeeds in characterizing both short- and long-range interactions in the presence of electrical charges
 220 utilizing additional interaction parameters.

221 The excess Gibbs free energy (G^E) NRTL expression modified for electrolyte systems is reported in the
 222 equation (20), where m stands for the generic neutral molecular species, c for cations, and a for anions. The

223 X_i (capital X) is defined in expression (21) as the product of the molar fraction of the generic species i (x_i)
 224 times a coefficient C_i which is assumed equal to unity for neutral molecules and to the absolute value of the
 225 charge for the ions (Lin et al., 2010). We remark that expressions (18) and (19) of the general NRTL model are
 226 still valid for electrolyte systems, and the parameters A_{ij} and B_{ij} in the equation (19) are called GMELCC and
 227 GMELCD parameters in Aspen Plus, respectively. The latter ones define the temperature dependence for
 228 anion/cation - molecule pairs interactions.

$$\frac{G^E}{RT} = \sum_m X_m \cdot \frac{\sum_j X_m \cdot G_{jm} \cdot \tau_{jm}}{\sum_k X_k \cdot G_{jk}} + \sum_c X_c \cdot \frac{\sum_{a'} \frac{X_{a'} \cdot \sum_j G_{j,c,a'} \cdot \tau_{j,c,a'}}{(\sum_{a''} X_{a''}) \cdot \sum_k X_k \cdot G_{k,c,a'}}}{\sum_a X_a \cdot \frac{\sum_{c'} \frac{X_{c'} \cdot \sum_j G_{j,a,c'} \cdot \tau_{j,a,c'}}{(\sum_{c''} X_{c''}) \cdot \sum_k X_k \cdot G_{k,a,c'}}} \quad (20)$$

$$X_i = x_i \cdot C_i \quad (21)$$

229 2.4.3 System speciation

230 Differently from soft models, which typically deal only with neutral molecules (amines, water and CO₂) and
 231 cannot distinguish between an amine and its protonated form, the ELECNRTL model is a true composition
 232 model since it is able to fully describe the composition of the system in the liquid phase including the single
 233 cationic and ionic species, the so-called speciation. The characterization of the liquid composition is provided
 234 by means of reaction equilibrium constants and the activity coefficients (see section 2.4.1). Such an increased
 235 level of detail allows a better understanding of the system, in particular the estimation of the relative content
 236 of bicarbonate and carbamate, which are forming as a result of two competitive reactions, and the
 237 thermodynamic behavior in solution (Richner and Puxty, 2012). Furthermore, by monitoring the speciation
 238 in CO₂ absorption/desorption processes, information on amine structure relationships, reaction mechanisms,
 239 influences of process operating conditions, and a deeper understanding of the absorption kinetics of the
 240 blend can be gathered (Perinu et al., 2018).

241 For chemical absorption of CO₂ by aqueous amine solvents, the most widely adopted technique to identify
 242 and quantify the species formed as a result of interactions between the unloaded solution and CO₂ is NMR
 243 spectroscopy (Chen et al., 2022). For the HS3 blend, no speciation data have been collected so far, meaning
 244 that a direct comparison between experimental liquid speciation and liquid speciation predicted by the VLE
 245 model is not possible. Anyway, the HS3 speciation as predicted by the new ELECNRTL model is presented in
 246 section 3.7 together with a list of considerations based on the published literature on AP and PRLD and in-
 247 house absorption heat data for HS3 that justify the observed behavior, at least from a qualitative point of
 248 view.

249 2.5 Physical properties

250 A proper carbon capture process design requires the characterization of the fluidodynamics of the reacting
 251 systems, the correct estimation of the CO₂ capture plant energy requirements as well as the kinetics of
 252 absorption and desorption (Guo et al., 2019). Physical properties such as density, viscosity and heat capacity
 253 of both pure components and their blend have a not negligible influence. More specifically, some authors
 254 remark that the liquid-film coefficients for mass transfer and vapor liquid equilibrium depend on the solution
 255 density, viscosity, and surface tension. In turn, this influences also the mass transfer rates inside both the

256 absorber and the regenerator (Balchandani et al., 2022). Additionally, the pumping costs associated with
257 amine solvent are significantly influenced by the viscosity of the solvents. Finally, an incorrect estimate of
258 the amine heat capacities directly results in an inaccurate estimation of the contribution to the reboiler duty
259 given by the sensible heat required to heat the rich-solvent up to the bottom reboiler temperature. For all
260 these reasons, it is fundamental to properly fix density, viscosity and specific heat of all the molecules
261 involved in the system before proceeding with the regression of the VLE interaction parameters.

262 Aspen Plus V11.0 allows fitting temperature dependent density, viscosity and heat capacity models for pure
263 component and both temperature and loading-dependent expressions based on dedicated mixing rules to
264 characterise amine-water mixtures (Aspen Plus®, 2019). In this work, literature data have been exploited to
265 regress dedicated density, viscosity and specific heat polynomials for pure AP and PRLD (Hartono and
266 Knuutia, 2023; Idris and Eimer, 2016; Idris et al., 2018; Mundhwa and Henni, A., 2007). Moreover, density
267 and viscosity observations for AP-water and PRLD-water solutions at different temperatures and
268 progressively increasing amine concentrations have been exploited to characterize amine densities and
269 viscosities at different molarities.

270 The density, viscosity and specific heat models obtained in this work and a comparison between the model
271 prediction and the corresponding experimental data are described in the Supplementary Material.

272

273 **2.6 General methodology to regress NRTL and ELECNRTL coefficients**

274

275 **2.6.1 NRTL VLE model: molecule-molecule interaction parameters**

276 Before moving to the definition and estimation of the ELECNRTL coefficients, it is important to fix the
277 equilibrium parameters for the uncharged blend, namely the equilibrium condition in the absence of CO₂.
278 Since the CO₂ is not dissolved into the solvent and no charged molecules are generated (except for water
279 self-ionization), the molecule-molecule interactions are the most relevant to describe the phase equilibria
280 established between the liquid and corresponding vapour. In general, the PRLD-H₂O and AP-H₂O interaction
281 parameters should be regressed using Aspen Plus V11 Regression toolbox with the "maximum likelihood"
282 algorithm starting from binary VLE experimental data. The regression is repeated using each time as a guess
283 value for the results of the previous iteration until the difference between two consecutive iterations is lower
284 than 0.1% for each parameter. The aim of this iterative procedure is to find the global optimum instead of
285 just a local minimum of the Sum of Square Errors (SSE) between each experimental datum and its model
286 prediction. In case of no or a few experimental data may be available for the amine-water system, it is worth
287 observing that the amine-water system equilibria are also present when CO₂ is dissolved. Thus, the amine-
288 CO₂-H₂O data can be used to get the NRTL coefficients as well.

289 For what concerns specifically the HS3 blend, the NRTL parameters had already been fitted on PRLD-H₂O VLE
290 data by Bernhardsen (Bernhardsen et al., 2019) and on AP-H₂O data by Bunevska (Bunevska, 2021). No
291 parameters accounting for AP-PRLD interactions have been considered since amine-amine interactions can
292 be neglected to increase the model robustness in accordance with all the other template ELECNRTL models
293 for amine blends proposed by AspenTach (Aspen Plus®, 2019). Amine-amine-water interaction parameters
294 could be regressed if blend-water equilibria data for unloaded solution are available. However, this kind of
295 data was not available for this system.

296

297 **2.6.2 ELECNRTL VLE model: ion-molecule interaction parameters**

298 The ELECNRTL package accounts for both long- and short-range interactions among molecules and pairs of
299 cations and anions. The electrostatic interactions are relevant in the liquid phase since the physical

300 entanglement between the different charged and uncharged molecules affects the activity of each species.
301 The regression of the ion-molecule interaction parameters has been carried out using experimental
302 measurements of the CO₂ partial pressure (PCO₂) at different loading [mol_{CO2}/mol_{amine}] data for the HS3 blend,
303 which is a quaternary system (AP-PRLD-H₂O-CO₂). In principle, AP-H₂O molecule-ion interaction coefficients
304 should be regressed starting from ternary AP-H₂O-CO₂ VLE data and the corresponding PRLD-H₂O interaction
305 from ternary VLE-H₂O-CO₂ data, while quaternary data should be used only to tune the AP-PRLD molecule-
306 ions interactions. This procedure would lead to a general model, valid for whatever relative content of AP,
307 PRLD and H₂O. Despite the advantage of getting a general model, this could lead to significantly higher errors
308 in the VLE prediction at the specific HS3 solvent composition. Since the main aim of this work is the
309 development of an accurate model to represent the HS3 solvent, the fitting has been done directly using only
310 quaternary HS3 data. This lead to a more accurate and reliable model for the considered blend. On the other
311 hand, there is no reliability in extrapolating the model for other amine concentration, which is underlined as
312 a limitation.

313 The general approach described in this section aims at providing a standard procedure to regress the
314 ELECNRTL parameters by reducing their amount to shorten and speed up calculations. The latter feature is
315 crucial since many regressed parameters guarantee numerical accuracy, whereas it may lead to convergence
316 issues when simulating an entire distillation/absorption column due to heavy computational efforts and high
317 potential correlation among the ELECNRTL parameters. Thus, a balanced trade-off between accuracy and the
318 number of parameters is required. The interaction parameters are classified in temperature non-dependent
319 parameters, denoted in Aspen Plus as GMELCC, corresponding to A_{ij} in Equation (19), and temperature-
320 dependent parameters, corresponding to GMELCD in Aspen and B_{ij} in Equation (19). To make the system as
321 simple as possible, it is worth looking first into the GMELCC, disregarding any temperature dependence. The
322 temperature dependence can be investigated separately. The best algorithm for the regression of the
323 ELECNRTL is the “maximum likelihood” (ML), which minimizes the gap between experimental observations
324 and model predictions changing the GMELCC (and GMELCD) parameters without fixing any variable
325 (temperature, pressure, liquid, and vapor composition). In other words, a multi-dimensional minimization
326 problem is solved. The experimental dataset should cover the entire range of temperatures and loading for
327 the domain of interest.

328 The complete procedure to regress the ELECNRTL parameter is here described:

- 329 1. As the first attempt, only the GMELCC (A_{ij}) are considered for the regression, and they are initially set
330 equal to their default values (Britt et al., 1982; Mouhoubi et al., 2020) ($A_{CO_2,ca}=15$, $A_{ca,CO_2}=-8$, $A_{amine,ca}=8$,
331 $A_{ca,amine}=-4$, $A_{H_2O,ca}=8$, $A_{ca,H_2O}=-4$, where c and a stand for a generic cation and anion, respectively). To
332 simplify the system, all the interactions of CO₂ as molecular species with the carbamate and the two
333 protonated amines are set equal to zero. Moreover, due to their low concentration (thus, negligible
334 molar fraction), any GMELCC parameters accounting for any interaction with H₃O⁺ as cation or OH⁻ and
335 CO₃⁻ as anion are not included in the regression procedure and they are fixed to the corresponding default
336 value when describing the interactions with water and equal to zero for the interactions with the two
337 amines. The proposed assumption is acceptable since the molar fraction of H₃O⁺ as cation or OH⁻ and
338 CO₃⁻ species is very low in amine systems, meaning that their impact on the activity coefficients in
339 equation (20) is negligible (Frailie et al., 2011; Li et al., 2014). The VLE model developed for HS3 confirms
340 this assumption, since the predicted mole fractions of the three mentioned ions ranges 10⁻⁴ – 10⁻⁹. As a
341 matter of fact, these species are diluted into the solvent and, according to the NRTL model, the activity
342 coefficient $\gamma_i \rightarrow 1$ (ideal liquid condition) and the VLE conditions are described by the Raoult model. The
343 remaining GMELCC are then regressed with the ML algorithm.
- 344 2. The regression procedure is repeated several times to try to ensure that a real optimum was found
345 instead of just a local minimum. More in detail, the regression procedure is repeated until further
346 iterative steps would result in negligible changes of all interaction parameters with respect to the

347 previous iteration (maximum relative discrepancy of 5% is accepted as a threshold). The resulting
 348 required number of iterations according to the mentioned criterion is 10. The results of each iteration
 349 are exploited as new guess starting values for the following one. The set of parameters with minimum
 350 square error and variance of the GMELCC is considered the optimal solution.

- 351 3. To improve the prediction capacity of the ELECNRTL model at high temperature, it is possible to include
 352 the GMELCD (B_{ij}) parameters which account for the temperature effect. Before starting, all the GMELCD
 353 to be regressed are set equal to zero (default value), and the GMELCC coefficients have been also reset
 354 to their default values. In the current work, we considered all the possible GMELCD parameters with a
 355 corresponding GMELCC regressed at point [1]. In other words, GMELCD considering H_3O^+ as cation or OH^-
 356 and CO_3^{2-} as anion in combination with the two amines were still disregarded.
- 357 4. To avoid overfitting and a vast number of ELECNRTL parameters, all GMELCD < 50.0 (in absolute value)
 358 after three iterations have been removed and fixed to zero.
- 359 5. Before the last regression, the remaining GMELCC and GMELCD parameters were reset to their default
 360 values. The ML algorithm has been applied ten times, and the solution showing the minimum sum of
 361 errors and variance has been chosen as the best.

362 Once the final model has been obtained, a point-to-point evaluation analysis using Aspen Plus V11 regression
 363 tool (in estimation mode) with the “ordinary least square” (OLS) algorithm has been performed to verify the
 364 experimental data matching and the accuracy of the model. This algorithm calculates the model prediction
 365 in terms of total pressure and vapour phase composition at fixed temperature and liquid composition. The
 366 statistical indicators, the average Relative Error (RE) and Average Absolute Error (AE) are used to assess
 367 the accuracy and the precision of the model. The accuracy is referred to the ability of a model to lie close to
 368 the experimental points, and the index of this feature is RE. The precision is related to the dispersion of the
 369 model and how much the results are distributed around the experimental observations (i.e., the precision of
 370 the model). The AE directly estimates this. The mean relative error (RE) is calculated according to Equation
 371 (22), where z stands for the variable on which the error is calculated (for example the pressure and molar
 372 fraction of water and PRLD in the vapor phase), i stands for the generic experimental point and n for the total
 373 number of measurements.

$$RE = \frac{1}{n} \cdot \sum_{i=1}^n \left| \frac{z_{i,exp} - z_{i,mod}}{z_{i,exp}} \right| \quad (22)$$

374
 375 The overall absolute error (AE) is instead defined according to Equation (23):

$$AE = \sqrt{\frac{\sum_{i=1}^n (z_{i,exp} - z_{i,mod})^2}{n}} \quad (23)$$

376
 377 It is remarkable that for an amine blend the maximum number of possible ELECNRTL parameters is

$$\frac{3n_M!}{n_M - 2} + 5n_M n_C n_A \quad (24)$$

378 where n_M , n_C , and n_A are the number of molecules, cations, and anions, respectively. Thus, for an amine blend
 379 made up of a primary amine and a tertiary amine, it is possible to define up to 276 coefficients (considering
 380 both GMELCC and GMELCD and neglecting pair cation-anion interactions). Such a high number of parameters
 381 results in overfitting and could lead to high correlation among the parameters. The suggested numerical
 382 procedure reduces by almost 88% the number of ELECNRTL regressed coefficients without appreciable loss

383 in accuracy. For instance, for the HS3 blend, we defined globally 34 ELECNRTL parameters subdivided into 24
384 GMELCC and 10 GMELCD. Thus, the proposed approach intrinsically helps define a codified procedure
385 reducing the number of parameters and focusing on the most relevant parameters.

386

387 **2.7 CO2SIM soft model (comparative model)**

388 Finally, we compared the VLE equilibrium results from the ELECNRTL model implemented in Aspen Plus V11
389 with the ones obtained from CO2SIM, for the specific blend. CO2SIM is a standalone software developed in
390 SINTEF Industry – Process Technology department to generate and simulate amine-based capture plants. The
391 CO2SIM software has been successfully implemented and validated over several pure amine and amine
392 blends (Lindqvist et al., 2014; Majeed and Svendsen, 2018; Pinto et al., 2014; Tobiesen et al., 2018, 2008,
393 2007). Differently from the Aspen Plus suite, CO2SIM for this particular solvent describes the VLE adopting
394 soft model approach (Brüder et al., 2012), in a so-called non-rigorous manner. In CO2SIM's chosen soft
395 equilibrium model, the partial pressure of the CO₂ in the gas phase (P_{CO_2}) in equilibrium with the liquid solvent
396 is defined as a function of the solvent loading (α) and temperature. The soft model structure has been largely
397 discussed and presented in previously cited works. Concerning the general structure, the soft model has
398 some adaptative coefficients (k-parameters, B, and C) which are fitted to the experimental data for an
399 assigned blend:

$$\ln(P_{CO_2}[\text{kPa}]) = B \cdot \ln(\alpha) + A_1 + \frac{C}{1 + A_2 \cdot \exp[-A_3 \cdot \ln(\alpha)]} \quad (25)$$

400 Despite the absence of a true thermodynamic framework, the soft model ensures good accuracy without any
401 numerical effort. Although speciation models are available in CO2SIM, the main advantage of the much used
402 soft models lies in the possibility to easily get fast calculations and to catch the main dependence of the
403 dependent variable (i.e., the partial pressure of free CO₂ in the gas phase) just considering the main system
404 variables as the solution loading and the temperature. Thus, the soft VLE model is empirically based on a
405 loading- and temperature-dependent terms, and it represents a smart short-cut for a fast representation of
406 experimental VLE data and interpretation of the amine/blend performance. The limited validity range (i.e.,
407 unfeasible extrapolation of the model outside the regression domain) represents the main drawback of the
408 soft model. Moreover, this soft model defines the HS3 as a pseudo component, thus, it is not able to
409 distinguish between the two single amine constituents. These limitations are related to the absence of a real
410 phenomenological and physics-based model, like the ELECNRTL theory.

411 **2.8 Heat of absorption**

412 The reaction between CO₂ and an amine solution is an exothermic process, thus it is associated with the
413 release of a certain quantity of heat, resulting in a system temperature increase. The amount of heat released
414 during the CO₂ absorption process is called the heat of absorption. This thermal energy depends on the
415 solvent formulation, the CO₂ loading and the temperature. A correct estimation of the heat of absorption for
416 acid gases (mainly CO₂ and H₂S) in aqueous amines solutions is of prime importance for designing unit
417 operations of acid gas removal, because it directly affects the steam requirements associated with amine
418 regeneration and its connection to the temperature dependency of the CO₂ equilibrium (Kim and Svendsen,
419 2011). On the one hand it is advisable to keep the absorption enthalpy as low as possible, as the steam cost
420 often accounts for over half the operating cost of the plant. On the other hand, this may negatively affect the
421 capture performance within the absorber. Even if the temperature dependency of the heat of absorption is
422 sometimes neglected assuming a constant value both for absorber and desorber conditions (Kohl and
423 Nielsen, 1997), experimental observations show that differences between the reaction heat estimate at 40°C

424 and at 120°C can reach 25–30% (Kim and Svendsen, 2011). Furthermore, accounting also for the dependency
 425 on the loading can lead to improvements in the correct optimal design of a CO₂ capture facility. Based on
 426 these considerations, it is essential for models to be implemented in process simulators to correctly predict
 427 absorption heat in the whole temperature and loading ranges of interest in order to guarantee a reasonable
 428 estimation of the energy requirements of the CO₂ capture plant and, as a consequence, of the operating
 429 costs.

430 The absorption heat associated with the reaction between CO₂ and the HS3 blend has been determined in a
 431 temperature range between 40°C and 100°C and in a CO₂ loading range between 0.03 and 0.81 employing a
 432 reaction calorimeter (Hartono et al.).

433 In this work, the available experimental observations for the primary and tertiary amine protonation heat
 434 and carbamate formation have been used to tune the Aspen ELECNRTL model to get an accurate estimation
 435 of the HS3 absorption heat. A comparison between the experimental data and the resulting model prediction
 436 is shown in section 3.8 to verify the reliability of the new proposed model. The following sub-paragraph
 437 provides an overview of the theoretical framework followed by Aspen Plus to estimate the reaction heat
 438 starting from the enthalpy of formation and the ideal gas, liquid, and diluted aqueous phase heat capacities
 439 of each molecular and ionic species involved in the reacting system. This section also describes the procedure
 440 that can be followed to estimate enthalpy of formation or heat capacity data for which no experimental
 441 observations are available, starting from the heat of absorption data. The proposed approach is applicable
 442 for the characterization of absorption heat in whatever blend.

443 2.8.1 Enthalpy calculations in Aspen Plus

444 In a default ELECNRTL package, the enthalpy of a particular species at a given temperature (T) is calculated
 445 according to expression (26) for a neutral molecule (H_{molecule}) and according to expression (27) for ions (H_{ion}),
 446 where the liquid (cP_{liq}) and aqueous (cP_{aq}) heat capacities are defined as a function of the temperature
 447 through expressions (28) and (29), respectively.

$$H_{\text{molecule}}(T) = \Delta H_{\text{f gas}}^0(298.15\text{K}) - \Delta H_{\text{ev}}(298.15\text{K}) + \int_{298.15\text{K}}^T cP_{\text{liq}} \cdot dT \quad (26)$$

448

$$H_{\text{ion}}(T) = \Delta H_{\text{faq}}^0(298.15\text{K}) + \int_{298.15\text{K}}^T cP_{\text{aqueous}} dT \quad (27)$$

449

$$cP_{\text{liq}} = A + B \cdot T + CT^2 + D \cdot T^3 + \frac{E}{T^2} \quad (28)$$

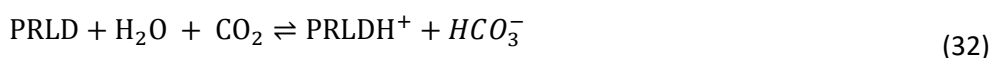
450

$$cP_{\text{aq}} = A + B \cdot T \quad (29)$$

451 In absence of specific calorimetric data on ionic species heat capacity, the aqueous heat capacity of
 452 protonated amines can be set equal to the corresponding pure amine liquid heat capacity to simplify
 453 calculations. Pure amines liquid heat capacities have been fitted to published experimental data for both AP
 454 and PRLD (see Supplementary Material). The ideal gas enthalpy of formation of CO₂ and H₂O as well as the
 455 aqueous enthalpy of formation of CO₃⁻, HCO₃⁻, H₃O⁺ and OH⁻ are available in the Aspen database and have
 456 been used successfully to characterize many amine systems (Aspen Plus®, 2019). Therefore, the only
 457 unknown parameters in expressions (26) to (29) are the enthalpies of the formation of pure and protonated
 458 AP and PRLD as well as the carbamate formation enthalpy. The formation enthalpy of AP and PRLD can be
 459 approximately estimated by means of Gani group contribution method (Constantinou and Gani, 1994). The

460 estimated values are comparable to those reported in the MEA-MDEA Aspen Plus V11.0 framework. The
 461 remaining formation enthalpies of APH^+ , $APCOO^-$ and $PRLDH^+$ can be regressed from absorption heat data at
 462 a fixed temperature (no loading dependence). Considering the definition of reaction heat reported in
 463 expression (30), where θ is the stoichiometric coefficient, a minimization problem is solved to calculate the
 464 optimal $\Delta H_f^0, APH^+$ from the AP protonation (r_4) reaction heat (Bunevska, 2021), $\Delta H_f^0, APHCOO^-$
 465 and $\Delta H_f^0, PRLDH^+$ from global CO_2 absorption reactions (31) and (32), respectively, starting from in-house
 466 absorption heat data determined for pure AP and pure PRLD-based solvents, respectively.

$$\Delta H^R(T) = \sum_{i=1}^{N_{products}} \Delta H_{f,i}^0(T) \cdot \vartheta_i - \sum_{j=1}^{N_{reactants}} \Delta H_{f,j}^0(T) \cdot \vartheta_j \quad (30)$$



468

469 3 RESULTS AND DISCUSSION

470 In this section, we present the results obtained by applying the guidelines proposed in the Methods
 471 paragraph.

472 3.1 Henry constants

473 Table 2 lists the values of parameters A, B, C and D for the Henry constant (He) of CO_2 in both pure amines
 474 as in Equation (2). Their values result from the minimization of the relative square deviations between the
 475 solubility calculated based on the experimental solubility data and the model predictions. Figure 2 shows the
 476 graphical comparison of the CO_2 solubility data rescaled according to the N_2O solubility analogy. The model
 477 proves accurate in the whole temperature range of interest and the model has a reasonable shape also at
 478 high temperatures where there is no experimental data available.

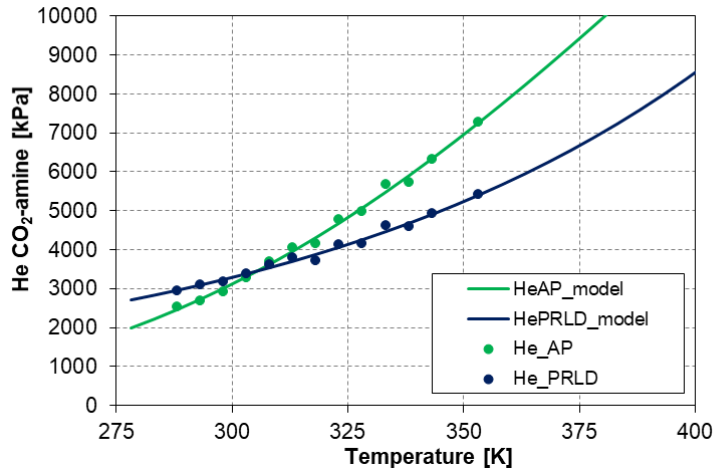
479

480

481 **Table 2. Henry law constant coefficients defining CO_2 physical solubility in AP and PRLD regressed in this work.**

Parameter	CO_2 - AP	CO_2 - PRLD
A	-54.6317	10.9911
B	-2.0334	0.3802
C	12.1097	-1.1906
D	-0.0213	0.0130

482



483

484 Figure 2. Henry law constant defining CO₂ physical solubility in AP and PRLD: model (solid line) and experimental data (dots).

485

486 **3.2 Vapor pressure**

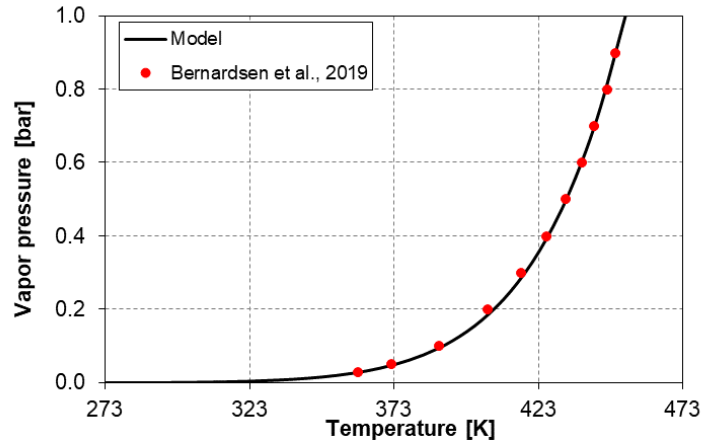
487 Antoine equation parameters C_1 , C_2 and C_3 (refer to Equation (4)) are already available in the literature for
 488 AP (Green and Perry, 2007), but they have been refitted in order to get an expression where coefficients are
 489 compliant with the unit of measure implemented in Aspen Plus and reported in Equation (4). Conversely, the
 490 coefficients of the PRLD have been fitted in this work to the vapor pressure data collected in Bernhardsen
 491 (Bernhardsen et al., 2019). A sum of relative square errors of only 0.7% is obtained. Antoine equation
 492 parameters regressed in this contribution and a comparison between the experimental PRLD vapor pressure
 493 data collected in the literature and the model prediction are provided in Table 3 and Figure 3, respectively.

494

495 Table 3. Antoine coefficients for AP and PRLD vapor pressures fitted (vapor pressure in [bar] and temperature in [K]).

Parameter	AP	PRLD
C_1	11.9628	20.3877
C_2	-4482.90	-12733.55
C_3	-85.50	171.53

496



497

498 **Figure 3. PRLD vapor pressure: experimental data (Bernardsen et al., 2019) and predictions using Antoine model.**

499

500 **3.3 Equilibrium constants of the elementary reactions scheme**

501 The equilibrium constants for the elementary reactions (5) - (10) have been taken from the literature. For the
 502 AP protonation and AP global reaction with CO₂ (expressions (8) and (9)), Dong et al. (Dong et al., 2010)
 503 provided a loading-dependent equilibrium constant expression. This has been reformulated and regressed
 504 into the Aspen Plus complaint form reported in Equation (11). Table 4 lists the coefficients for equilibrium
 505 constants of the elementary reactions adopted to describe the CO₂ capture using the HS3 blend as solvent.

506

507

508

509

510

511 **Table 4. Coefficients for molar fraction-based equilibrium constants according to expression (11).**

	r₁ Equation (5)	r₂ Equation (6)	r₃ Equation (7)	r₄ Equation (8)	r₅ Equation (9)	r₆ Equation (10)
A	132.899	231.465	216.049	-106.105	1.21526	-10.4165
B	-13445.9	-12092.1	-12431.7	-4134.2	-1068.67	-4234.98
C	-22.4773	-36.7816	-35.4819	16.2313	-	-
D	-	-	-	-	-	-
Source	(Posey and Rochelle, 1997)	(Posey and Rochelle, 1997)	(Posey and Rochelle, 1997)	Refitted from Dong (Dong et al., 2010)	Refitted from Dong (Dong et al., 2010) and Rochelle (Posey and Rochelle, 1997)	Calculated from Li et al., 2017

512

513 **3.4 NRTL model coefficients (molecule-molecule interactions)**

514 Table 5 gathers the NRTL coefficients for the H₂O-AP and H₂O-PRLD interactions as available in the literature.

515

516 Table 5. NRTL parameters implemented in Aspen Plus for the molecule - molecule interactions

Aspen Plus NRTL coefficient	Parameters in expressions (18) and (19)	Component i	Component j	Value (SI units)	Source of experimental values
NRTL/1	A_{ij}	H ₂ O	AP	5.3843	(Bunevska, 2021)
NRTL/2	B_{ij}	H ₂ O	AP	-0.9199	
NRTL/1	A_{ji}	AP	H ₂ O	-989.213	
NRTL/2	B_{ji}	AP	H ₂ O	-440.101	
NRTL/3	$\alpha_{ij} = \alpha_{ji}$	H ₂ O	AP	0.2	
NRTL/1	A_{ij}	H ₂ O	PRLD	1.1755	(Bernhardsen et al., 2019)
NRTL/2	B_{ij}	H ₂ O	PRLD	-0.1156	
NRTL/1	A_{ji}	PRLD	H ₂ O	-1103.81	
NRTL/2	B_{ji}	PRLD	H ₂ O	1715.89	
NRTL/3	$\alpha_{ij} = \alpha_{ji}$	H ₂ O	PRLD	0.2	

517

518 3.5 ELECRTL model coefficients (molecule - anion/cation pairs interactions)

519 Table 6 gathers the values for the regressed ELECRTL model (both GMELCC and GMELCD). The coefficients
520 missing in this list are set to their default values or to zero, as mentioned in the methodology proposed in
521 Section 2.6.2.

522

523

524 Table 6. ELECRTL coefficients (GMELCC and GMELCD) implemented in Aspen Plus to characterize pure amines and the HS3 blend.
525 The table reports only the coefficients which are not set to default values.

ELECRTL coefficient Aspen Plus name	Element i	Element j	Value (SI units)
GMELCC	H ₂ O	(PRLDH ⁺ ,HCO ₃ ⁻)	13.6961
GMELCC	(PRLDH ⁺ ,HCO ₃ ⁻)	H ₂ O	-5.4276
GMELCC	PRLD	(PRLDH ⁺ ,HCO ₃ ⁻)	29.0442
GMELCC	(PRLDH ⁺ ,HCO ₃ ⁻)	PRLD	8.7717
GMELCC	H ₂ O	(APH ⁺ ,HCO ₃ ⁻)	12.6182
GMELCC	(APH ⁺ ,HCO ₃ ⁻)	H ₂ O	-5.5317
GMELCC	H ₂ O	(APH ⁺ ,APCOO ⁻)	10.5229
GMELCC	(APH ⁺ ,APCOO ⁻)	H ₂ O	-6.9975
GMELCC	AP	(APH ⁺ ,HCO ₃ ⁻)	87.2557
GMELCC	(APH ⁺ ,HCO ₃ ⁻)	AP	60.3790
GMELCC	AP	(APH ⁺ ,APCOO ⁻)	20.7888
GMELCC	(APH ⁺ ,APCOO ⁻)	AP	34.8014
GMELCC	H ₂ O	(PRLDH ⁺ ,APCOO ⁻)	10.9464
GMELCC	(PRLDH ⁺ ,APCOO ⁻)	H ₂ O	-5.1289
GMELCC	AP	(PRLDH ⁺ ,HCO ₃ ⁻)	52.3316
GMELCC	(PRLDH ⁺ ,HCO ₃ ⁻)	AP	35.0286
GMELCC	AP	(PRLDH ⁺ ,APCOO ⁻)	4.5923

GMELCC	(PRLDH ⁺ , APCOO ⁻)	AP	-1.3794
GMELCC	PRLD	(PRLDH ⁺ , APCOO ⁻)	12.5491
GMELCC	(PRLDH ⁺ , APCOO ⁻)	PRLD	2.8911
GMELCC	PRLD	(APH ⁺ , HCO ₃ ⁻)	11.6230
GMELCC	(APH ⁺ , HCO ₃ ⁻)	PRLD	0.1155
GMELCC	PRLD	(APH ⁺ , APCOO ⁻)	7.4596
GMELCC	(APH ⁺ , APCOO ⁻)	PRLD	19.9230
GMELCD	PRLD	(PRLDH ⁺ , HCO ₃ ⁻)	888.2463
GMELCD	(PRLDH ⁺ , HCO ₃ ⁻)	PRLD	8810.9267
GMELCD	AP	(APH ⁺ , HCO ₃ ⁻)	1959.2531
GMELCD	(APH ⁺ , HCO ₃ ⁻)	AP	1514.6851
GMELCD	AP	(APH ⁺ , APCOO ⁻)	-259.7171
GMELCD	(APH ⁺ , APCOO ⁻)	AP	432.8310
GMELCD	AP	(PRLDH ⁺ , APCOO ⁻)	530.2970
GMELCD	(PRLDH ⁺ , APCOO ⁻)	AP	-789.5392
GMELCD	PRLD	(PRLDH ⁺ , APCOO ⁻)	-2337.3930
GMELCD	(PRLDH ⁺ , APCOO ⁻)	PRLD	-66.6320

526

527 Finally, the authors performed a statistical analysis of the results over the different datasets we used for the
528 regression of the ELECNRTL coefficients. Table 7 resumes the performance of the regression for the data
529 clusters. The statistical analysis neglects the amines partial pressure due to its low numerical value which is
530 not relevant to the present discussion. Thus, the error analysis is limited to CO₂ and water vapor partial
531 pressure, which represent the main components present in the vapor phase. Overall, the statistical analysis
532 shows good accuracy and precision of the model, since the average relative errors are below 20% and the
533 absolute deviations are close to 7 kPa. Such results confirm the reliability of the regression procedure
534 presented in this contribution. The largest deviations are registered for the predictions of the CO₂ partial
535 pressure data. These deviations are enhanced by the fact that a significant number of experimental data
536 report a very low measured partial pressure of CO₂. Thus, even though the absolute value may be close to
537 the experimental one (as shown by looking at the average AE), the relative error increases. For this reason,
538 the relative error on CO₂ partial pressure calculated accounting only for the data associated with a CO₂ partial
539 pressure higher than 1 kPa is also included in the statistical analysis. The results demonstrate that it is possible
540 to build up an ELECNRTL model from scratch even though one or more components making up the blend are
541 missing in the defaults Aspen Plus database.

542

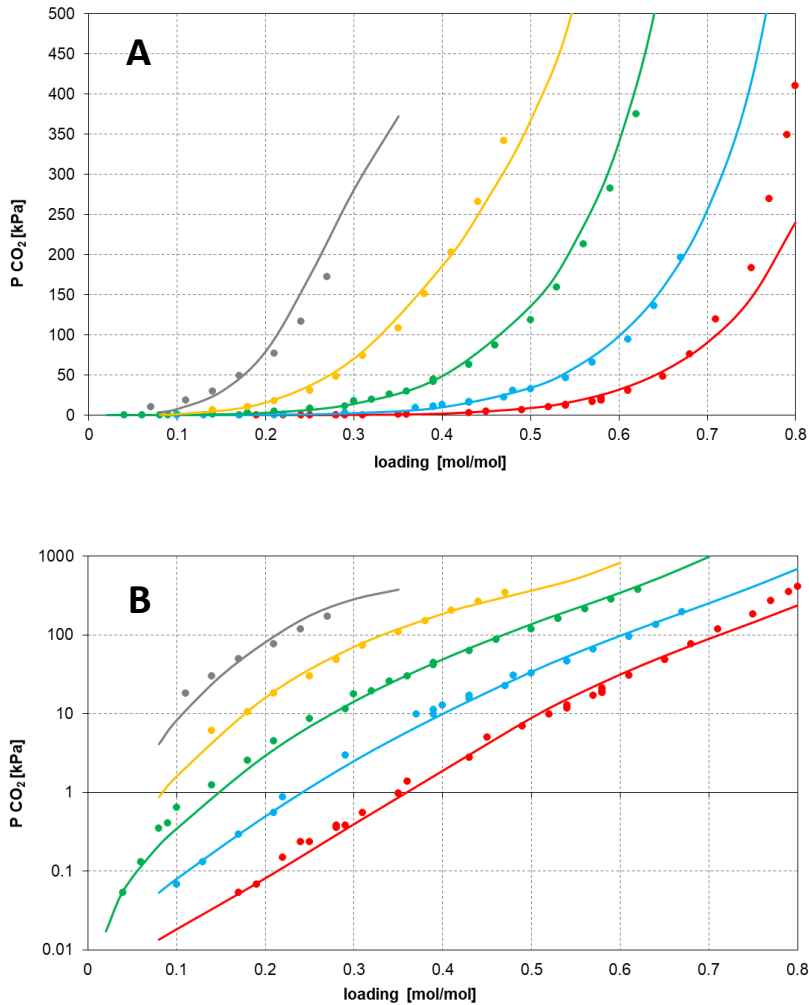
543 **Table 7. Average AE and RE of CO₂ and water partial pressure predictions for the ELECNRTL and CO2SIM models for HS3 developed**
544 **in this work and corresponding experimental data available in the literature for the AP-PRLD-H₂O-CO₂ system (HS3 blend).**

Model	Data source	Chart (P _{CO2} vs loading)	RE [%] as in Equation (22)		AE [bar] as in Equation (23)	
			P _{CO2}	P _{H2O}	P _{CO2}	P _{H2O}
ELECNRTL	Hartono et al.	Figure 4	17.84	17.00	0.0712	0.0705
ELECNRTL	Hartono et al. only data with P _{CO2} > 1 kPa	Figure 4	14.81	-	-	-
CO2SIM	Hartono et al.	Figure S8 and S9	14.29	-	0.214	-

545

546

547 Figure 4 depicts the VLE curves for the HS3 blend over different loading at different temperatures, which are
 548 the most relevant for CCS plant. The Aspen Plus ELECNRTL model shows good accuracy in representing the
 549 equilibrium conditions in the whole temperature (40°C-120°C) and loading (0.1 – 0.5) range of interest for
 550 both absorption and solvent regeneration (Dutcher et al., 2015; Liu et al., 2016; Mangalapally and Hasse,
 551 2011; Rao and Rubin, 2002; Rochelle, 2009). Moreover, it is possible to claim that the model can be
 552 extrapolated since the profiles are smooth and no abnormal trends are registered. For a comparison between
 553 ELECNRTL model and the soft model developed in CO2SIM, please refer to the following paragraph.



554

555

556 **Figure 4. Comparison between the ELECNRTL model predictions (solid lines) and the experimental data (dots) for the HS3 blend at**
 557 **different temperatures: 40°C (red), 60°C (light blue), 80°C (green), 100°C (yellow), and 120°C (grey). The plot is proposed both in**
 558 **normal scale (A - top) and logarithmic (B - bottom). Data by Hartono (Hartono et al.).**

559

560 3.6 Comparison of the Aspen Plus ELECNRTL model with the CO2SIM soft model

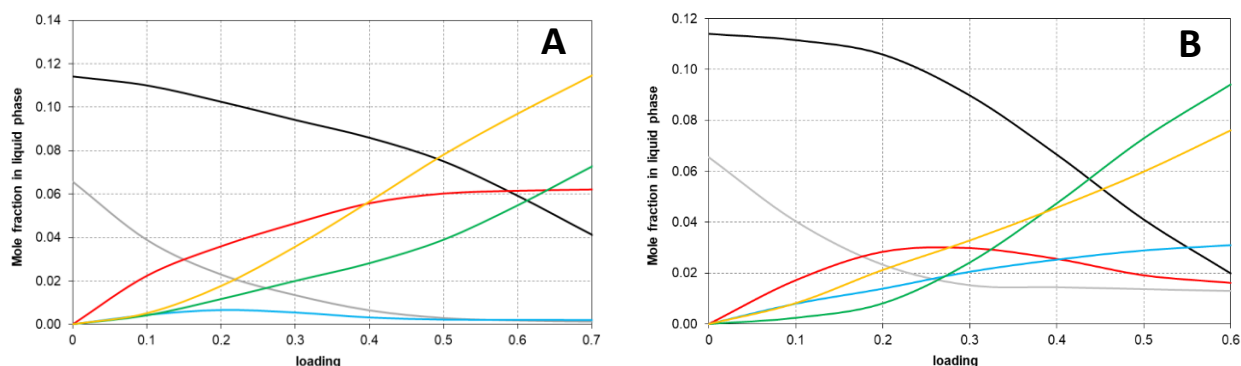
561 We compared the ELECNRTL model with the soft model implemented in the in-house CO2SIM process
 562 simulator. The necessity to verify the reliability of the ELECNRTL model drives the choice of comparing two
 563 different models, one theory-based (Aspen ELECNRTL) and one empirical (CO2SIM soft model). We
 564 considered the CO2SIM model as a benchmark since previous works (Brüder et al., 2011) proved that CO2SIM
 565 soft model represents accurately and with precision amine(s) VLE as already mentioned in Section 2.7. The
 566 coefficients of the empirical CO2SIM soft VLE model have been regressed to define the CO₂ partial pressure's
 567 dependency on loading and temperature for the HS3 blend allowing a comparison of two models for the HS3

568 blend. A graphical comparison between the ELECNRTL and the CO2SIM model can be found in the
 569 Supplementary Material. The ELECNRTL model is associated with a slightly higher relative error but also with
 570 (Brüder et al., 2011) a significantly lower (-66%) absolute error (Table 7). This result is in some way expected,
 571 considering that the algorithm exploited for the regression procedure in Aspen Plus V11.0 is based on the
 572 minimization of the absolute deviations between the experimental data and the model prediction. The
 573 CO2SIM soft VLE model looks smoother, but only the Aspen ELECNRTL model can differentiate between the
 574 two amine constituents (AP and PRLD), while the soft model deals with a pseudo component including both
 575 amines together. Therefore, under proper validation with additional experimental data, the Aspen ELECNRTL
 576 model can be extended to describe not only the specific HS3 blend composition but also whatever solvent
 577 composition between pure ternary AP-H₂O-CO₂ and pure PRLD-H₂O-CO₂ systems. Finally, conversely to the
 578 soft model, which does not take into account the formation of cations and anions in the system, the ELECNRTL
 579 model provides details concerning the composition of the liquid phase at equilibrium (speciation).

580

581 3.7 Speciation in the liquid phase

582 The speciation of the reacting system in the liquid phase as predicted by the VLE model obtained within this
 583 article is shown in Figure 5 at a temperature of 40°C and 120°C as a function of the CO₂ loading. These
 584 temperatures have been selected since they represent the operating conditions typical of the two most
 585 important unit operations in the CO₂ capture process, namely CO₂ absorption and solvent regeneration,
 586 respectively. In the absence of experimental data, it is possible only to make some qualitative considerations
 587 on the obtained speciation plots and to compare the results with the corresponding speciation provided by
 588 Aspen Plus for another primary-tertiary amine blend, namely MEA-MDEA (Figure 6), at the same weight
 589 solvent composition (15 wt% primary amine, 40 wt% tertiary amine).

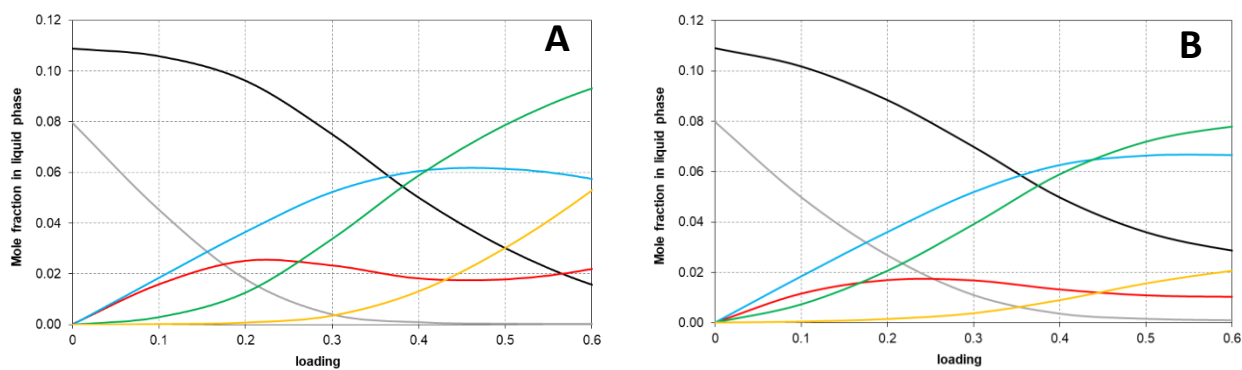


590

591 **Figure 5. Speciation in the liquid phase predicted by the Aspen Plus ELECNRTL model for HS3 as a function of loading at 40°C (A)**
 592 **and 120°C (B): AP (grey), PRLD (black), APH+ (red), APCOO- (light blue), PRLDH+ (green) and HCO₃- (yellow).**

593

594



595

596 **Figure 6. Speciation in the liquid phase predicted by the Aspen Plus ELECNRTL default model as a function of loading at 40°C (A)**
 597 **and 120°C (B) for the MEA-MDEA blend: MEA (grey), MDEA (black), MEAH+ (red), MEACOO- (light blue), MDEAH+ (green) and**
 598 **HCO₃⁻ (yellow).**

599

600 As expected, the primary amine is more reactive than the tertiary amine at low loadings (<0.2), thus it is
 601 consumed faster. At higher loadings, PRLD becomes more active than the primary amine, which is associated
 602 with an increase in the overall CO₂ absorption capacity of the system. As the tertiary amines reacts, PRLDH⁺
 603 and HCO₃⁻ are progressively formed, while the products of AP conversion are APH⁺ and APCOO⁻. Differently
 604 from common primary amines such as MEA, which tends to easily form carbamate rather than being
 605 protonated, for the HS3 blend amine protonation seems to be favored, thus limiting carbamate formation.
 606 In both systems, the carbamate formation reaches a peak at intermediate loadings at low temperature, while
 607 it increases until it reaches a steady state value at 120°C. In addition, differently from MDEA, the tertiary
 608 amine selected for this blend formulation (PRLD) is very reactive also at high temperature, which is an
 609 additional reason for the quite rapid increase in the bicarbonate formation observed both at 40°C and at
 610 120°C. These observations can be justified in light of the outcomes of published experimental work.
 611 (Benamor et al., 2015) have demonstrated that AP equilibrium protonation constant is almost 6% higher with
 612 respect to the corresponding MEA protonation constant. Moreover, the experimental PRLD protonation
 613 constant determined by Liu et al., 2016 is, on average, 5.6 times higher with respect to the MDEA protonation
 614 constant, and the discrepancy becomes more pronounced at increasing temperatures, which is a
 615 confirmation of the higher reactivity of PRLD with respect to benchmark tertiary amines. As for the reaction
 616 heat, a value close to 100 kJ/mole CO₂ which remains constant when the loading lies between 0 and 0.4 is
 617 observed for pure AP solution (Bunevska, 2021), while the absorption heat for PRLD is 34 kJ/mol (Liu et al.,
 618 2016). In systems where the primary amine is much more reactive than the tertiary one, a quite flat
 619 absorption heat profile at low loadings is also observed for the blend (for example in the MEA-MDEA system).
 620 In other words, when the carbamate formation dominates over the bicarbonate formation the heat of
 621 absorption remains almost constant with the loading, while this is not the case when the most significant
 622 contribution is associated with bicarbonate formation. The sudden decrease observed for HS3 absorption
 623 heat data at low loadings may thus be motivated by the fact that in this system the bicarbonate formation,
 624 in which PRLD plays the key role, becomes competitive even at low loadings, meaning that carbamate
 625 formation is not favoured. This behaviour may explain the observed differences in the HS3 speciation plots
 626 with respect to the ones associated with the MEA-MDEA reference system.

627

628 **Heat of absorption**

629 Table 8 gathers the formation enthalpies for AP, PRLD and their corresponding ionic species estimated within
 630 this work following the methodology highlighted in section 2.8.1.

631 By adding those input data to the Aspen model, enthalpy calculations can be performed. Indeed, Aspen Plus
 632 calculates the specific enthalpy of a mixture of n components (H_{mix}) as the sum of an ideal mixture term,
 633 where x_i is the mole fraction and H_i the pure component specific enthalpy, and an enthalpy departure term
 634 (H_{mix}^E), whose value is calculated from the activity coefficient (see expression (33)).

$$H_{\text{mix}} = \sum_{i=1}^n x_i \cdot H_i + H_{\text{mix}}^E \quad (33)$$

635 The reliability of the energy calculations is checked in Figure 7 by comparing the experimental heat of
 636 absorption of CO_2 data for HS3 with the corresponding absorption heat predicted by the model in the whole
 637 temperature and CO_2 loading range of interest.

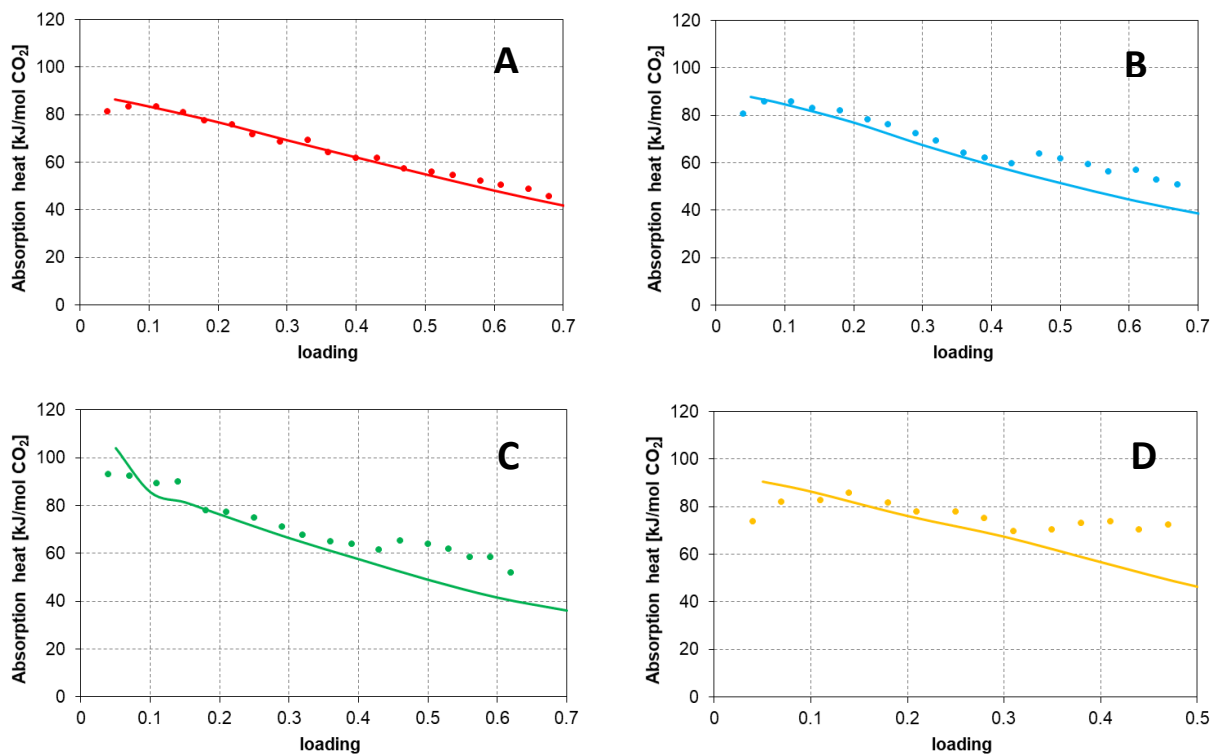
638

639

640 Table 8. Enthalpy of formation of amines, protonated amines and AP carbamate estimated within this work.

Species	ΔH_f^0 [kJ/mol]	Phase
AP	-225.172	Ideal gas
PRLD	-223.147	Ideal gas
APH ⁺	-313.002	Aqueous
APCOO ⁻	-732.771	Aqueous
PRLDH ⁺	-300.003	Aqueous

641



642

643

644 Figure 7. Comparison between the Aspen Plus ELECRTL model predictions (solid lines) and the experimental data (dots) for the
 645 HS3 blend absorption heat at different temperatures: 40°C (A), 60°C (B), 80°C (C) and 100°C (D). Data by Hartono (Hartono et al.).

646 The model provides a very accurate estimation of the heat of absorption of CO_2 at 40°C (operating conditions
 647 of interest for the absorber) in the entire investigated loading range. When the temperature increases, the
 648 ELECRTL model is still accurate in predicting the heat of absorption at low CO_2 loading (0.1 – 0.4), while at

649 higher loadings an apparent underestimation is observed. However, a trend showing a progressive
650 monotonic reduction of the absorption heat at high loadings, as the one shown by the model, is more realistic
651 and compatible with similar trends observed for other amine systems (Kim et al., 2014, 2009). The only
652 reasonable explanation for an absorption heat trend with a double peak like the one in Figure 7 B) to D) is
653 the presence of a region at intermediate loadings where some precipitation occurs (Kim and Svendsen, 2011).
654 Since precipitation would not be expected in any of the experimental campaigns carried out at NTNU and
655 SINTEF Industry with HS3, the uncommon trend in experimental heat of absorption at high loadings may be
656 associated with experimental inaccuracies, while the trend predicted by the model remains physically
657 meaningful in the whole investigated temperature and loading range.

658

659

660 **3.8 Statistics of the regression in Aspen Plus (correlation coefficients analysis)**

661 Finally, we also performed a statistical analysis on the regressed ELECNRTL parameters (GMELCC and
662 GMELCD) to estimate the correlations among these coefficients. The values of the Correlation Coefficients
663 (CoCos) have been directly obtained using the Aspen Plus regression tool. The results are plotted in Figure 8.
664 The CoCos matrix (Figure 8A) enables identifying any potential correlations between the regressed
665 parameters. Linear correlation negatively affects the regression, and it would lead to an overfitting problem
666 which is reflected in stability issues of the ELECNRTL model while solving VLE calculations in flash and
667 absorber/stripper. The CoCos matrix is symmetric and, for this reason, only the left-hand side is reported.
668 The matrix considers all the possible combinations of the ELECNRTL coefficients (both GMELCC and GMELCD)
669 among the 34 coefficients listed in Table 6. All the elements on the diagonal are self-coupled elements, thus
670 by definition, their CoCos are equal to one. However, the elements on the main diagonal are not relevant to
671 the statistical analysis. All the relevant CoCos lie out of the diagonal. When the value of the CoCo approaches
672 the unit, the two parameters are fully linearly dependent, meaning that there is a strong mutual dependence.
673 When CoCo is close to -1, the two coefficients are perfectly anti-correlated, but also in this case there is a
674 strong mutual influence between the two. As a rule of thumb, low values for the CoCos are desired (i.e., close
675 to zero). There is no clear standard indication of which threshold values for the CoCo have been defined to
676 state the correlation between a couple of regressed parameters. The Kirk-Othmer encyclopaedia (Buzzi-
677 Ferraris and Manenti, 2011) just reports some general guidelines (not values), and in the literature, there are
678 no published works suggesting how to handle the CoCo matrix. Further details are reported on websites
679 dedicated to statistical analysis (Andrews.edu, accessed November 2022).

680 The statistical analysis of the CoCos matrix is reported both in Figure 8B and

681 Table 9. The results show that the CoCos are normally distributed around the expected null value, and only
682 a few are strongly correlated or anti-correlated. This means that the proposed retrofit procedure avoids
683 potential correlation issues which may lead to model instabilities. Furtherly, according to the statistical
684 analysis, 94.5% of the coefficients are $|\text{CoCo}| < 0.5$, which represents the threshold value to define a weak
685 and almost negligible correlation. In case a more conservative range is considered, 88.8% and 82.2% of the
686 coefficients still lies within the domain $|\text{CoCo}| < 0.4$ and $|\text{CoCo}| < 0.3$, respectively. These results furtherly
687 confirm the previous comments and point out that correlation does not represent any relevant issue for the
688 proposed model.

Range	Occurrence	Frequency
from -1.00 to -0.90	6	1.07%
from -0.90 to -0.80	2	0.36%
from -0.80 to -0.70	5	0.89%
from -0.70 to -0.60	0	0.00%
from -0.60 to -0.50	7	1.25%
from -0.50 to -0.40	14	2.50%
from -0.40 to -0.30	16	2.85%
from -0.30 to -0.20	58	10.34%
from -0.20 to -0.10	70	12.48%
from -0.10 to -0.00	112	19.96%
from 0.00 to 0.10	119	21.21%
from 0.10 to 0.20	70	12.48%
from 0.20 to 0.30	32	5.70%
from 0.30 to 0.40	21	3.74%
from 0.40 to 0.50	15	2.67%
from 0.50 to 0.60	6	1.07%
from 0.60 to 0.70	0	0.00%
from 0.70 to 0.80	0	0.00%
from 0.80 to 0.90	2	0.36%
from 0.90 to 1.00	6	1.07%

691

692
693

694

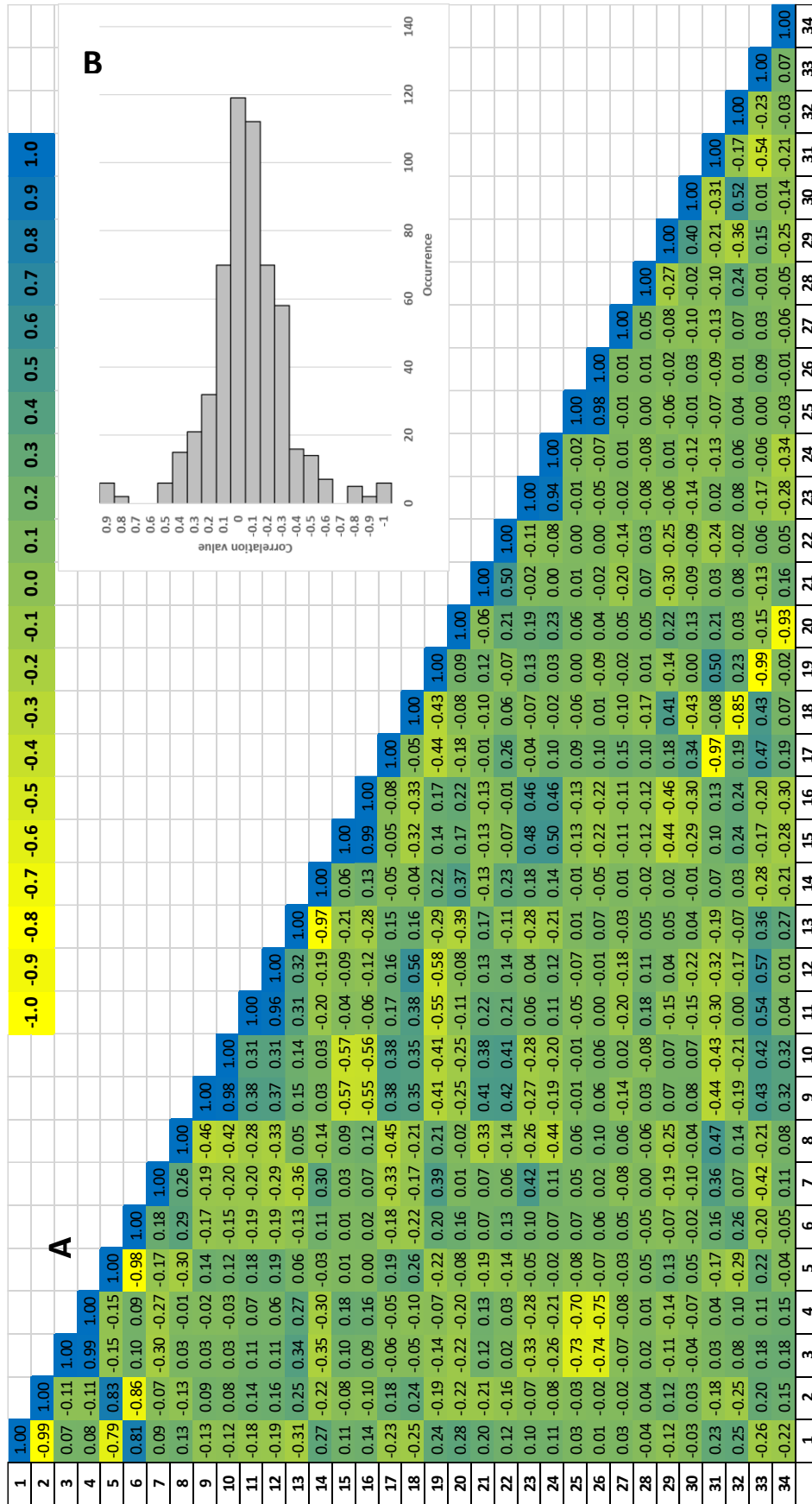


Figure 8. Results of the correlation analysis of the regressed parameters: triangular correlation matrix and relative colour bar scale (A) and the distribution of the correlation coefficients (B).

695 **4 Conclusions**

696 A detailed general procedure to be followed for the implementation of a new amine-blend model in Aspen
697 Plus® has been presented. Thus, the proposed approach can be applied to any system where the NRTL and
698 ELECNRTL parameters for the activity coefficient should be defined and regressed using experimental data.

699 Physical CO₂ solubility in an aqueous AP and PRLD blend has been modelled by means of the Henry's constant,
700 which has been fitted to experimental data collected by exploiting the N₂O analogy. The reaction scheme
701 characterizing the primary and tertiary amine interactions with water and CO₂ are defined in compliance with
702 previous models available in Aspen Plus for similar amine blends, while the corresponding equilibrium
703 constants are collected from the literature. ELECNRTL interaction parameters are fitted to in-house VLE data
704 for the HS3 solvent.

705 The comparison with the experimental data shows that the proposed ELECNRTL model enables predicting
706 VLE with good accuracy. In particular, the new model can predict CO₂ partial pressure with an average relative
707 deviation lower than 18% with respect to all VLE data and lower than 15% if considering the data with partial
708 pressure of CO₂ higher than 1 kPa. The average absolute deviation is limited to 7 kPa. The ELECNRTL model
709 here proposed turns out to be valid under a wide range of temperatures and CO₂ loading, which covers the
710 whole range of operating conditions of interest for both CO₂ absorption and amine regeneration. The
711 proposed model is reliable, providing also insights into the liquid speciation. Furthermore, the Aspen model
712 can be extended to handle both pure amines and their blends since each amine is fully defined as a real
713 component.

714 The proposed model can predict with high accuracy the absorption heat in the whole investigated
715 temperature (40°C to 100°C) and CO₂ loading (0.03 to 0.7) ranges. This means that the model can be exploited
716 to reasonably estimate the energy requirements and the operating costs of a CO₂ capture plant based on
717 HS3. In addition, the regressed Aspen model provides a reasonable liquid phase speciation which is in line
718 with the observations arising from previous experimental studies carried out with AP and PRLD systems as
719 well as with the HS3 absorption heat in-house data. Finally, a statistical analysis of the correlation coefficients
720 among the interaction parameters demonstrates that no relevant overfitting issues occur, which is important
721 to guarantee the stability of the obtained model.

722 Dedicated physical property model parameters have been regressed to allow a proper description of the
723 main AP and PRLD properties such as density, viscosity, and specific heat in the liquid phase (see
724 Supplementary Material). Where possible, the fitting procedure is based on both in-house and published
725 data. Interactions between water and amines have also been considered in the regression of water-amine
726 mixtures density and viscosity models. All the property models show appreciable accuracy at all investigated
727 temperatures and compositions.

728

729 **Fundings**

730 This work was performed within REALISE project. The project has received funding from the European
731 Union's Horizon 2020 research and innovation programme under grant agreement No 884266 (REALISE
732 project). For more information refers to the project webpage - [Home | REALISE-CCUS \(realiseccus.eu\)](https://realiseccus.eu)

733

734

735

736

737 **References**

- 738 Andrews.edu, n.d. Correlation Coefficients [WWW Document].
739 <https://www.andrews.edu/~calkins/math/edrm611/edrm05.htm>
- 740 Aronu, U.E., Gondal, S., Hessen, E.T., Haug-Warberg, T., Hartono, A., Hoff, K.A., Svendsen, H.F., 2011.
741 Solubility of CO₂ in 15, 30, 45 and 60 mass% MEA from 40 to 120°C and model representation using
742 the extended UNIQUAC framework. *Chem Eng Sci* 66, 6393–6406.
743 <https://doi.org/10.1016/j.ces.2011.08.042>
- 744 Aspen Plus®, 2019. Aspen Plus® V11.0 Documentation.
- 745 Balchandani, S.C., Dey, A., Mandal, B., Kumar, A., Dharaskar, S., 2022. Elucidating the important thermo
746 physical characterization properties of amine activated hybrid novel solvents for designing post-
747 combustion CO₂ capture unit. *J Mol Liq* 355. <https://doi.org/10.1016/j.molliq.2022.118919>
- 748 Benamor, A., Al-Marri, M.J., Hawari, A., 2015. Experimental determination of carbamate formation and
749 amine protonation constants in 3-amino-1-propanol-CO₂-H₂O system and their temperature
750 dependency. *International Journal of Greenhouse Gas Control* 37, 237–242.
751 <https://doi.org/10.1016/j.ijggc.2015.03.026>
- 752 Bernhardsen, I.M., Trollebø, A.A., Perinu, C., Knuutila, H.K., 2019. Vapour-liquid equilibrium study of
753 tertiary amines, single and in blend with 3-(methylamino)propylamine, for post-combustion CO₂
754 capture. *Journal of Chemical Thermodynamics* 138, 211–228.
755 <https://doi.org/10.1016/j.jct.2019.06.017>
- 756 Bishnoi, S., Rochelle, G.T., 2000. Physical and chemical solubility of carbon dioxide in aqueous
757 methyldiethanolamine, *Fluid Phase Equilibria*.
- 758 Bisotti, F., Fedeli, M., Prifti, K., Galeazzi, A., Dell'Angelo, A., Manenti, F., 2022. Impact of Kinetic Models on
759 Methanol Synthesis Reactor Predictions: In Silico Assessment and Comparison with Industrial Data.
760 *Ind Eng Chem Res* 61, 2206–2226. <https://doi.org/10.1021/acs.iecr.1c04476>
- 761 Bisotti, F., Galeazzi, A., Galatioto, L., Masserdotti, F., Bigi, A., Gritti, P., Manenti, F., 2021. Implementing
762 robust thermodynamic model for reliable bubble/dew problem solution in cryogenic distillation of air
763 separation units. *International Journal of Thermofluids* 10. <https://doi.org/10.1016/j.ijft.2021.100083>
- 764 Britt, H. 1, Boston, J.F., Evans, L.B., 1982. Local Composition Model for Excess Gibbs Energy of Electrolyte
765 Systems Part I: Single Solvent, Single Completely Dissociated Electrolyte Systems CHAU-CHYUN CHEN,
766 *AIChE Journal*.
- 767 Brúder, P., Grimstvedt, A., Mejdell, T., Svendsen, H.F., 2011. CO₂ capture into aqueous solutions of
768 piperazine activated 2-amino-2-methyl-1-propanol. *Chem Eng Sci* 66, 6193–6198.
769 <https://doi.org/10.1016/j.ces.2011.08.051>
- 770 Brúder, P., Lauritsen, K.G., Mejdell, T., Svendsen, H.F., 2012. CO₂ capture into aqueous solutions of 3-
771 methylaminopropylamine activated dimethyl-monoethanolamine. *Chem Eng Sci* 75, 28–37.
772 <https://doi.org/10.1016/j.ces.2012.03.005>
- 773 Bunevska, T., 2021. Characterization of a solvent for chemical absorption-based CO₂ capture.
- 774 Buzzi-Ferraris, G., Manenti, F., 2011. Data Interpretation and Correlation, in: *Kirk-Othmer Encyclopedia of*
775 *Chemical Technology*. pp. 1–33. <https://doi.org/https://doi.org/10.1002/0471238961.databuzz.a01>

776 Chen, C.-C., Song, Y., 2004. Generalized electrolyte-NRTL model for mixed-solvent electrolyte systems.
777 *AIChE Journal* 50, 1928–1941. <https://doi.org/https://doi.org/10.1002/aic.10151>

778 Chen, Guangying, Chen, Guangjie, Peruzzini, M., Zhang, R., Barzagli, F., 2022. Understanding the potential
779 benefits of blended ternary amine systems for CO₂ capture processes through ¹³C NMR speciation
780 study and energy cost analysis. *Sep Purif Technol* 291. <https://doi.org/10.1016/j.seppur.2022.120939>

781 Constantinou, L., Gani, R., n.d. New Group Contribution Method for Estimating Properties of Pure
782 Compounds.

783 Dong, L., Chen, J., Gao, G., 2010. Solubility of carbon dioxide in aqueous solutions of 3-amino-1-propanol,
784 in: *Journal of Chemical and Engineering Data*. pp. 1030–1034. <https://doi.org/10.1021/jc900492a>

785 Dutcher, B., Fan, M., Russell, A.G., 2015. Amine-based CO₂ capture technology development from the
786 beginning of 2013-A review. *ACS Appl Mater Interfaces* 7, 2137–2148.
787 <https://doi.org/10.1021/am507465f>

788 epa.gov, 2022. Overview of Greenhouse Gases [WWW Document].

789 Frailie, P., Plaza, J., van Wagener, D., Rochelle, G.T., 2011. Modeling piperazine thermodynamics, in: *Energy*
790 *Procedia*. Elsevier Ltd, pp. 35–42. <https://doi.org/10.1016/j.egypro.2011.01.020>

791 Green, D., Perry, R., 2007. *Perry's chemical engineer's handbook*, 8th Edition. ed. McGraw-Hill Education.

792 Guo, H., Hui, L., Shen, S., 2019. Monoethanolamine+2-methoxyethanol mixtures for CO₂ capture: Density,
793 viscosity and CO₂ solubility. *Journal of Chemical Thermodynamics* 132, 155–163.
794 <https://doi.org/10.1016/j.jct.2018.12.028>

795 Hartono, A., Ahmad, R., Svendsen, H.F., Knuutila, H.K., 2021. New solubility and heat of absorption data for
796 CO₂ in blends of 2-amino-2-methyl-1-propanol (AMP) and Piperazine (PZ) and a new eNRTL model
797 representation. *Fluid Phase Equilib* 550. <https://doi.org/10.1016/j.fluid.2021.113235>

798 Hartono, A., Carusone, F., Knuutila, H. Equilibrium behavior and the heat of absorption of CO₂ of aqueous 3-
799 amino-1-propanol and 3-amino-1-propanol - 1-(2-hydroxyethyl) pyrrolidine blends. Under preparation
800 to be submitted

801 Kim, I., Hoff, K.A., Hessen, E.T., Haug-Warberg, T., Svendsen, H.F., 2009. Enthalpy of absorption of CO₂ with
802 alkanolamine solutions predicted from reaction equilibrium constants. *Chem Eng Sci* 64, 2027–2038.
803 <https://doi.org/10.1016/j.ces.2008.12.037>

804 Kim, I., Hoff, K.A., Mejdell, T., 2014. Heat of absorption of CO₂ with aqueous solutions of mea: New
805 experimental data, in: *Energy Procedia*. Elsevier Ltd, pp. 1446–1455.
806 <https://doi.org/10.1016/j.egypro.2014.11.154>

807 Kim, I., Svendsen, H.F., 2011. Comparative study of the heats of absorption of post-combustion CO₂
808 absorbents. *International Journal of Greenhouse Gas Control* 5, 390–395.
809 <https://doi.org/10.1016/j.ijggc.2010.05.003>

810 'Kohl, A., "Nielsen Richard," 1997. *Gas Purification*, Fifth Edition. ed. Gulf Professional Publishing.

811 Kucka, L., Müller, I., Kenig, E.Y., Górak, A., 2003. On the modelling and simulation of sour gas absorption by
812 aqueous amine solutions. *Chem Eng Sci* 58, 3571–3578. [https://doi.org/10.1016/S0009-](https://doi.org/10.1016/S0009-2509(03)00255-0)
813 [2509\(03\)00255-0](https://doi.org/10.1016/S0009-2509(03)00255-0)

814 Li, H., Frailie, P.T., Rochelle, G.T., Chen, J., 2014. Thermodynamic modeling of piperazine/2-
815 aminomethylpropanol/CO₂/water. *Chem Eng Sci* 117, 331–341.
816 <https://doi.org/10.1016/j.ces.2014.06.026>

817 Li, M., Liu, H., Luo, X., Tontiwachwuthikul, P., Liang, Z., 2017. Development of Ion Speciation Plots for Three
818 Promising Tertiary Amine-CO₂-H₂O Systems Using the pH Method and the ¹³C NMR Method. *Energy*
819 and Fuels 31, 3069–3080. <https://doi.org/10.1021/acs.energyfuels.6b03320>

820 Lin, Y., ten Kate, A., Mooijer, M., Delgado, J., Fosbøl, P.L., Thomsen, K., 2010. Comparison of activity
821 coefficient models for electrolyte systems. *AIChE Journal* 56, 1334–1351.
822 <https://doi.org/10.1002/aic.12040>

823 Lin, Y.-J., Hsieh, C.-J., Chen, C.-C., 2022. Association-based activity coefficient model for electrolyte
824 solutions. *AIChE Journal* 68, e17422. <https://doi.org/https://doi.org/10.1002/aic.17422>

825 Lindqvist, K., Jordal, K., Haugen, G., Hoff, K.A., Anantharaman, R., 2014. Integration aspects of reactive
826 absorption for post-combustion CO₂ capture from NGCC (natural gas combined cycle) power plants.
827 *Energy* 78, 758–767. <https://doi.org/10.1016/j.energy.2014.10.070>

828 Liu, H., Chen, G., Liang, Z., 2016. Toward rational selection of amine solutions for PCC applications: CO₂
829 absorption kinetics and absorption heat in tertiary aqueous solutions. *International Journal of*
830 *Greenhouse Gas Control* 50, 206–217. <https://doi.org/10.1016/j.ijggc.2016.04.020>

831 Majeed, H., Svendsen, H.F., 2018. Effect of water wash on mist and aerosol formation in absorption
832 column. *Chemical Engineering Journal* 333, 636–648. <https://doi.org/10.1016/j.ces.2017.09.124>

833 Mangalapally, H.P., Hasse, H., 2011. Pilot plant study of two new solvents for post combustion carbon
834 dioxide capture by reactive absorption and comparison to monoethanolamine. *Chem Eng Sci* 66,
835 5512–5522. <https://doi.org/10.1016/j.ces.2011.06.054>

836 Mouhoubi, S., Dubois, L., Loldrup Fosbøl, P., de Weireld, G., Thomas, D., 2020. Thermodynamic modeling of
837 CO₂ absorption in aqueous solutions of N,N-diethylethanolamine (DEEA) and N-methyl-1,3-
838 propanediamine (MAPA) and their mixtures for carbon capture process simulation. *Chemical*
839 *Engineering Research and Design* 158, 46–63. <https://doi.org/10.1016/j.cherd.2020.02.029>

840 Pellegrini, L.A., Gilardi, M., Giudici, F., Spatolisano, E., 2021. New solvents for CO₂ and H₂S removal from
841 gaseous streams. *Energies (Basel)* 14. <https://doi.org/10.3390/en14206687>

842 Perinu, C., Bernhardsen, I.M., Pinto, D.D.D., Knuutila, H.K., Jens, K.J., 2018. NMR Speciation of Aqueous
843 MAPA, Tertiary Amines, and Their Blends in the Presence of CO₂: Influence of pK_a and Reaction
844 Mechanisms. *Ind Eng Chem Res* 57, 1337–1349. <https://doi.org/10.1021/acs.iecr.7b03795>

845 Pinto, D.D.D., Knuutila, H., Fytianos, G., Haugen, G., Mejdell, T., Svendsen, H.F., 2014. CO₂ post combustion
846 capture with a phase change solvent. Pilot plant campaign. *International Journal of Greenhouse Gas*
847 *Control* 31, 153–164. <https://doi.org/10.1016/j.ijggc.2014.10.007>

848 Posey, M.L., Rochelle, G.T., 1997. A Thermodynamic Model of Methyl-diethanolamine-CO₂-H₂O-Water.

849 Rao, A.B., Rubin, E.S., 2002. A technical, economic, and environmental assessment of amine-based CO₂
850 capture technology for power plant greenhouse gas control. *Environ Sci Technol* 36, 4467–4475.
851 <https://doi.org/10.1021/es0158861>

852 REALISE, 2022. REALISE CCUS [WWW Document].

853 Renon, H., Prausnitz, J.M., 1969. Estimation of Parameters for the NRTL Equation for Excess Gibbs Energies
854 of Strongly Nonideal Liquid Mixtures. *Industrial & Engineering Chemistry Process Design and*
855 *Development* 8, 413–419. <https://doi.org/10.1021/i260031a019>

856 Renon, H., Prausnitz, J.M., 1968. Local compositions in thermodynamic excess functions for liquid mixtures.
857 *AIChE Journal* 14, 135–144. <https://doi.org/https://doi.org/10.1002/aic.690140124>

858 Richner, G., Puxty, G., 2012. Assessing the chemical speciation during CO₂ absorption by aqueous amines
859 using in situ FTIR. *Ind Eng Chem Res* 51, 14317–14324. <https://doi.org/10.1021/ie302056f>

860 Rochelle, G.T., 2009. Amine Scrubbing for CO₂ Capture. *Science* (1979).
861 <https://doi.org/10.1126/science.1176731>

862 Sada, E., Kumzawa, H., Butt, M.A., 1977. Solubilities of Gases in Aqueous Solutions of Amine. *J Chem Eng*
863 *Data* 22.

864 Svendsen, H.F., Hessen, E.T., Mejdell, T., 2011. Carbon dioxide capture by absorption, challenges and
865 possibilities. *Chemical Engineering Journal* 171, 718–724. <https://doi.org/10.1016/j.cej.2011.01.014>

866 Tobiesen, F.A., Haugen, G., Hartono, A., 2018. A systematic procedure for process energy evaluation for
867 post combustion CO₂ capture: Case study of two novel strong bicarbonate-forming solvents. *Appl*
868 *Energy* 211, 161–173. <https://doi.org/10.1016/j.apenergy.2017.10.091>

869 Tobiesen, F.A., Juliussen, O., Svendsen, H.F., 2008. Experimental validation of a rigorous desorber model for
870 CO₂ post-combustion capture. *Chem Eng Sci* 63, 2641–2656.
871 <https://doi.org/10.1016/j.ces.2008.02.011>

872 Tobiesen, F.A., Svendsen, H.F., Juliussen, O., 2007. Experimental validation of a rigorous absorber model for
873 CO₂ postcombustion capture. *AIChE Journal* 53, 846–865. <https://doi.org/10.1002/aic.11133>

874 Yamada, H., 2021. Amine-based capture of CO₂ for utilization and storage. *Polym J* 53, 93–102.
875 <https://doi.org/10.1038/s41428-020-00400-y>

876